

Descending Control of Itch Transmission by the Serotonergic System via 5-HT1A-Facilitated GRP-GRPR Signaling

Zhong-Qiu Zhao,^{1,2,9} Xian-Yu Liu,^{1,2,9} Joseph Jeffry,^{1,2} W.K. Ajith Karunarathne,^{2,10} Jin-Lian Li,³ Admire Munanairi,^{1,2} Xuan-Yi Zhou,^{1,11} Hui Li,^{1,2,3} Yan-Gang Sun,^{2,12} Li Wan,^{1,2,13} Zhen-Yu Wu,³ Seungil Kim,^{2,14} Fu-Quan Huo,^{1,2,15} Ping Mo,^{1,2,4} Devin M. Barry,^{1,2} Chun-Kui Zhang,³ Ji-Young Kim,² N. Gautam,^{2,5} Kenneth J. Renner,⁶ Yun-Qing Li,³ and Zhou-Feng Chen^{1,2,7,8,*}

¹Center for the Study of Itch, Washington University School of Medicine, St. Louis, MO 63110, USA

²Department of Anesthesiology, Washington University School of Medicine, St. Louis, MO 63110, USA

³Department of Anatomy, Histology and Embryology, K. K. Leung Brain Research Centre, The Fourth Military Medical University, Xi'an 710032, China

⁴Department of Anesthesiology, the Affiliated Nanhai Hospital of Southern Medical University, Foshan 528000, China

⁵Department of Genetics, Washington University School of Medicine, St. Louis, MO 63110, USA

⁶Department of Biology, University of South Dakota, Vermillion, SD 57069, USA

⁷Department of Psychiatry, Washington University School of Medicine, St. Louis, MO 63110, USA

⁸Department of Developmental Biology, Washington University School of Medicine, St. Louis, MO 63110, USA

⁹Co-first author

¹⁰Present address: Department of Chemistry and Biochemistry, The University of Toledo, Toledo, OH 43606, USA

¹¹Present address: College of Life Sciences, Wuhan University, Wuhan, Hubei 430072, China

¹²Present address: Institute of Neuroscience, Academy of Chinese Science, Shanghai 200031, China

¹³Present address: Department of Anesthesiology, The Second Affiliated Hospital, Guangzhou Medical University, Guangzhou 510260, China

¹⁴Present address: Department of Cell and Tissue Biology, Craniofacial and Mesenchymal Biology, University of California, San Francisco, CA 94143, USA

¹⁵Present address: Department of Physiology and Pathophysiology, Xi'an Jiaotong University School of Medicine, Xi'an, Shaanxi 710061, China

*Correspondence: chenz@wustl.edu

<http://dx.doi.org/10.1016/j.neuron.2014.10.003>

SUMMARY

Central serotonin (5-hydroxytryptophan, 5-HT) modulates somatosensory transduction, but how it achieves sensory modality-specific modulation remains unclear. Here we report that enhancing serotonergic tone via administration of 5-HT potentiates itch sensation, whereas mice lacking 5-HT or serotonergic neurons in the brainstem exhibit markedly reduced scratching behavior. Through pharmacological and behavioral screening, we identified 5-HT1A as a key receptor in facilitating gastrin-releasing peptide (GRP)-dependent scratching behavior. Coactivation of 5-HT1A and GRP receptors (GRPR) greatly potentiates subthreshold, GRP-induced Ca²⁺ transients, and action potential firing of GRPR⁺ neurons. Immunostaining, biochemical, and biophysical studies suggest that 5-HT1A and GRPR may function as receptor heteromeric complexes. Furthermore, 5-HT1A blockade significantly attenuates, whereas its activation contributes to, long-lasting itch transmission. Thus, our studies demonstrate that the descending 5-HT system facilitates GRP-GRPR signaling via 5-HT1A to augment itch-specific outputs, and a disruption of crosstalk

between 5-HT1A and GRPR may be a useful antipruritic strategy.

INTRODUCTION

Somatosensory integration and transduction in the spinal cord and the trigeminal brainstem are subject to monoaminergic modulation. As an integral part of an animal's adaptive response to an ever-changing environment, facilitatory and inhibitory modulation of somatosensory neural circuits is crucial for the maintenance of homeostasis. Monoaminergic modulation of neural circuits serves an important role in regulating behavioral responses to somatosensory inputs. One notable example is that an array of monoamine neuromodulators produced by supraspinal regions is important for the modulation of nociceptive transmission (Basbaum and Fields, 1984; Suzuki et al., 2004). Given the fundamental role of central modulation in sensory transduction, one can presume that itch sensation is similarly modulated at several levels. Imaging studies in human subjects indicated that pain-mediated inhibition of itch is associated with an activity level of the midbrain regions such as periaqueductal gray matter (PAG), an area known for pain modulation (Mochizuki et al., 2003). Experiments in humans also indicated that noxious counterirritants reduce itch sensation (Murray and Weaver, 1975; Ward et al., 1996; Yosipovitch et al., 2007). Interruption of the upper cervical spinal cord of rodents attenuated

dry skin-induced itch, suggesting an involvement of the descending spinal pathway in itch responses (Akiyama et al., 2011).

G protein-coupled receptors (GPCRs), or seven *trans*-membrane proteins, constitute a large repertoire of cellular sensors required for transducing sensory signals from the skin to the brain (Jeffrey et al., 2011; Julius and Nathans, 2012). Gastrin-releasing peptide receptor (GRPR) is a G_q protein-coupled receptor that belongs to the mammalian bombesin receptor family (Jensen et al., 2008; Kroog et al., 1995). GRPR is expressed in laminae I–II of spinal cord neurons and has an important role in the transmission of pruritogenic information (Liu et al., 2011; O'Donohue et al., 1984; Sun and Chen, 2007; Sun et al., 2009). Gastrin-releasing peptide (GRP), an endogenous neuropeptide for itch, is expressed in a subset of dorsal root ganglion (DRG) and trigeminal ganglion (TG) cells and mediates GRPR activation in the spinal cord (Sun and Chen, 2007; Takanami et al., 2014; Zhao et al., 2013). While confusion has arisen about GRP expression in DRG neurons, the issue has recently been clarified (Liu et al., 2014; Takanami et al., 2014; Zhao et al., 2013, 2014). The GRP-GRPR pathway is primarily engaged in transducing nonhistaminergic acute itch sensation and may play a relatively minor role in histaminergic itch (Akiyama et al., 2014; Sun et al., 2009; Zhao et al., 2014). Enhanced GRP and GRPR expression is positively correlated with the intensity of chronic itch manifested by increased scratching bouts of animals (Nattkemper et al., 2013; Tominaga et al., 2009; Zhao et al., 2013). Conversely, loss of GRPR or GRP markedly reduces chronic itch (Lagerström et al., 2010; Zhao et al., 2013), demonstrating the importance of GRPR in the development and maintenance of chronic itch. Despite these studies, molecular mechanisms by which the function of GRPR is modulated remain elusive.

Serotonergic neurons reside principally in the brainstem raphe nuclei and modulate a myriad of behavioral and physiological functions through descending and ascending pathways (Barnes and Sharp, 1999; Dillon et al., 2004). Serotonergic neurons in the rostral ventromedial medulla (RVM), including nucleus raphe magnus (NRM) and surrounding reticular formation, project to both the trigeminal nucleus caudalis (SpVc) and the dorsal horn of the spinal cord and modulate nociceptive transmission in a bidirectional fashion (Basbaum and Fields, 1984; Millan, 2002; Ossipov et al., 2010; Suzuki et al., 2004). In contrast to numerous studies of serotonergic modulation of pain, little is known about the involvement of central 5-HT and receptor mechanisms in itch modulation. In this study, we tested the hypothesis that 5-HT signaling has a pivotal role in itch modulation.

RESULTS

Central Serotonin Facilitates Itch Transmission Elicited by Chloroquine

To evaluate the involvement of the central serotonergic system in modulation of itch transmission, we first examined the scratching behavior of *Lmx1b^{fl/fl}* mice to intradermal injection (i.d.) of chloroquine (CQ), a representative nonhistaminergic pruritogen that acts, in part, via a Mas-related GPCR (MrgprA3) in sensory neurons and GRPR in the spinal cord (Liu et al., 2009; Sun and Chen, 2007). LMX1B is a LIM homeodomain-containing tran-

scription factor that is required for the development of all central 5-HT neurons (Ding et al., 2003). We previously generated conditional *Lmx1b^{fl/fl}* mice in which *Lmx1b* is conditionally ablated in *Pet1*-expressing serotonergic neurons in the raphe nuclei. As a result, all central 5-HT neurons of *Lmx1b^{fl/fl}* mice were ablated due to lack of *Lmx1b* (Zhao et al., 2006). However, these mice survive and exhibit normal motor function and thus represent a unique genetic model for investigating the role of central 5-HT neurons in diverse physiological functions (Zhao et al., 2007a, 2007b). Compared with wild-type (WT) mice, CQ-evoked scratching responses were significantly reduced in *Lmx1b^{fl/fl}* mice (Figure 1A), demonstrating that central 5-HT neurons exert a constitutive tone for positively modulating itch transmission. To determine whether the decrease was specifically due to a loss of 5-HT or whether other factors originating in central 5-HT neurons were involved, we generated mice lacking tryptophan hydroxylase 2 (*Tph2*), which encodes the rate-limiting enzyme for 5-HT synthesis in the brain (Walther et al., 2003) using gene targeting strategy (Figure 1B). *Tph2^{-/-}* mice showed no expression of *Tph2* and 5-HT in the central nervous system but maintained normal presumptive 5-HT neurons (Figure 1B) (Kim et al., 2014; Liu et al., 2011). *Tph2^{-/-}* mice displayed a significant reduction in scratching response after i.d. injection of CQ in nape models (Figure 1C), recapitulating the phenotype of *Lmx1b^{fl/fl}* mice. Since 5-HT signaling in the brain and the spinal cord may contribute differentially to the modulation of itch sensation, next we asked whether impaired itch sensation observed in *Lmx1b^{fl/fl}* mice and *Tph2^{-/-}* mice may be ascribed to a blockage of the descending 5-HT pathway. We selectively degenerated spinal 5-HT⁺ terminals in the spinal cord by an intrathecal injection (i.t.) of 5,7-dihydroxytryptamine (5,7-DHT) following pretreatment with desipramine to prevent the transport of 5,7-DHT into noradrenergic and dopaminergic terminals (Björklund et al., 1975). At 2 weeks after 5,7-DHT injection, when spinal 5-HT⁺ fibers were depleted (Figure S1A, available online), mice exhibited an attenuated scratching response to CQ (Figure 1D), mimicking the phenotype of *Lmx1b^{fl/fl}* mice and *Tph2^{-/-}* mice. These loss-of-function studies confirm the contribution of descending 5-HT signaling to the modulation of itch sensation.

To complement the loss-of-function approaches, we next determined whether we could rescue the attenuated itch transmission of *Tph2^{-/-}* mice and *Lmx1b^{fl/fl}* mice using an intraperitoneal (i.p.) injection of the 5-HT precursor, 5-hydroxytryptophan (5-HTP), to boost 5-HT tone. Exogenous 5-HTP can be decarboxylated to 5-HT by aromatic L-amino acid decarboxylase (AADC), thereby bypassing the need for TPH2 for 5-HT synthesis (Figure 1B) (Birdsall, 1998). Indeed, immunohistochemical staining (IHC) revealed abundant 5-HT staining in the spinal cord of *Tph2^{-/-}* mice after 5-HTP injection (Figure 1E, top panel). In contrast, *Lmx1b^{fl/fl}* mice treated with 5-HTP failed to produce 5-HT in the brain (Figure 1E, lower row). High-performance liquid chromatography (HPLC) analysis also revealed a significant increase in 5-HT concentrations and its metabolite, 5-hydroxyindoleacetic acid (5-HIAA), in the brain and spinal cord of *Tph2^{-/-}* and wild-type mice treated with 5-HTP (Figures S1B–S1E). These studies demonstrate a successful conversion of 5-HT from 5-HTP in the absence of TPH2 and that 5-HT synthesis is

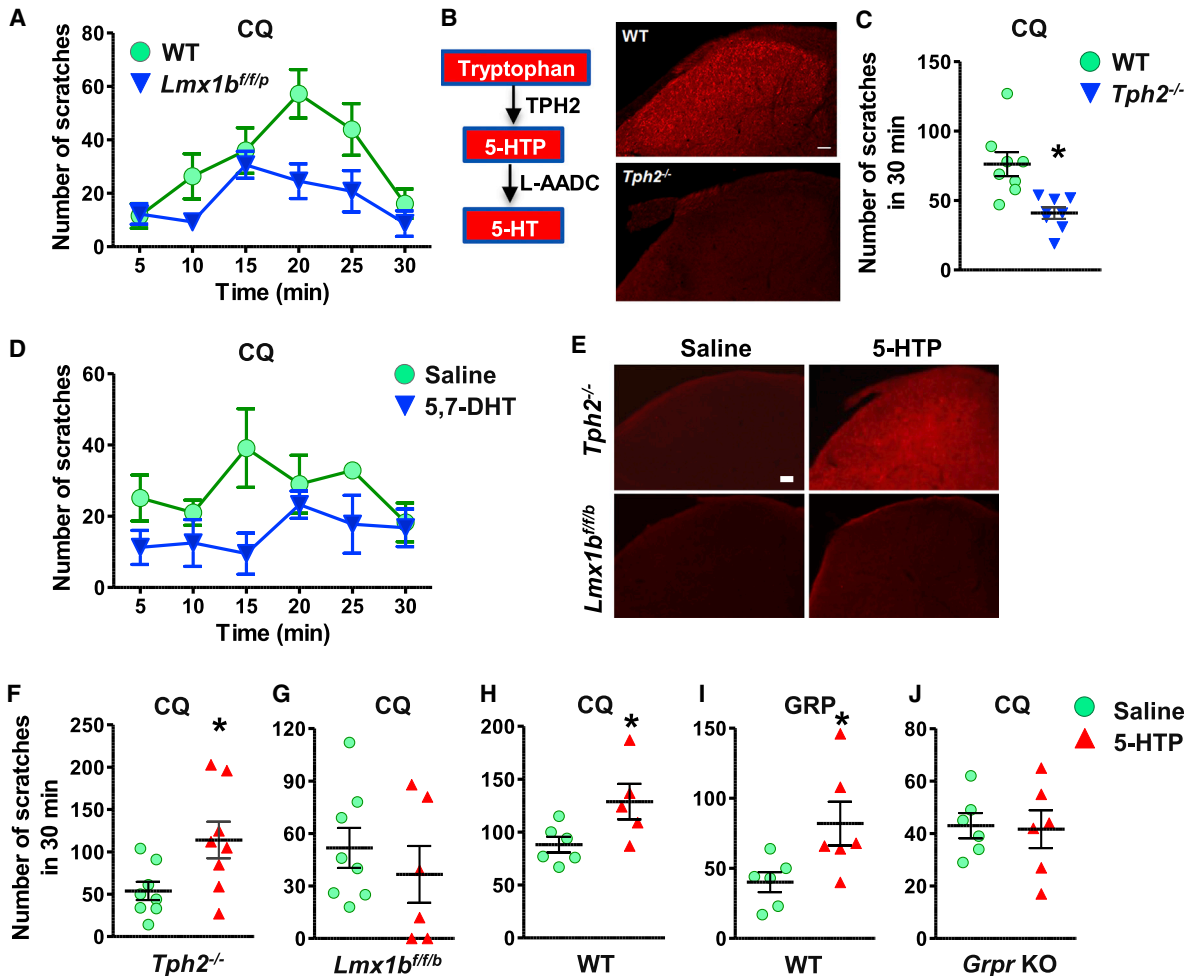


Figure 1. Central Serotonin Facilitates Itch Transmission

(A) *Lmx1b^{fl/flp}* mice showed deficits in CQ-induced scratching behavior ($p < 0.05$).

(B) Diagram showing synthesis of 5-HT in the brain. IHC images show that spinal 5-HT was not detectable in *Tph2^{-/-}* mice.

(C) *Tph2^{-/-}* mice exhibited attenuated CQ-induced scratching responses.

(D) CQ-induced scratching responses were attenuated after 5,7-DHT injection in C57Bl/6J mice ($p < 0.05$).

(E) Injection of 5-HTP (10 mg/kg, i.p.) for 60 min restored dorsal spinal 5-HT in *Tph2^{-/-}* mice, but not in *Lmx1b^{fl/flp}* mice.

(F and G) Injection of 5-HTP for 30 min rescued CQ-induced scratching behavior in *Tph2^{-/-}* mice (F), but not in *Lmx1b^{fl/flp}* mice (G).

(H–J) Injection of 5-HTP facilitated scratching behaviors induced by CQ (H) and GRP (I) in C57Bl/6J mice, while *Grpr* KO mice did not respond to 5-HTP injection (J).

Error bars represent SEM. * $p < 0.05$ versus WT (C) or saline (F–J), by unpaired t test in (C) and (F)–(J), or two-way repeated-measures ANOVA in (A) and (D). $n = 6–9$. Scale bars, 100 μm . See also Figure S1.

critically dependent on 5-HT neurons that express AADC. We next examined scratching responses of *Tph2^{-/-}* mice after 5-HTP injection and found that 5-HTP injection indeed restored normal scratching responses of *Tph2^{-/-}* mice to CQ (Figure 1F). However, the same treatment failed to enhance CQ-elicited scratching in *Lmx1b^{fl/flp}* mice (Figure 1G). This finding complements the results from the 5,7-DHT lesion study suggesting that 5-HT is important in the facilitation of CQ-induced itch and supports the notion that AADC in 5-HT neurons is required for catalyzing the conversion of 5-HTP into 5-HT. These results also demonstrate that peripheral 5-HT is not involved in modulation of itch transmission. Consistently, WT mice treated with

5-HTP showed a dramatic increase of CQ-elicited scratching (Figure 1H). Since CQ-elicited itch is dependent on GRP-GRPR signaling (Sun and Chen, 2007), we reasoned that 5-HT might synergistically act with GRP to enhance the function of GRPR. We tested this possibility by examining the GRP-induced scratching (GIS) with an intracisternal injection in mice treated with 5-HTP. Indeed, GIS was markedly potentiated by 5-HTP (Figure 1I), revealing a positive correlation between the activity of GRPR and central 5-HT tone. Importantly, 5-HTP injection did not affect the scratching response induced by CQ in *Grpr* KO mice (Figure 1J). Taken together, we conclude that spinal 5-HT signaling facilitates itch transmission through GRPR.

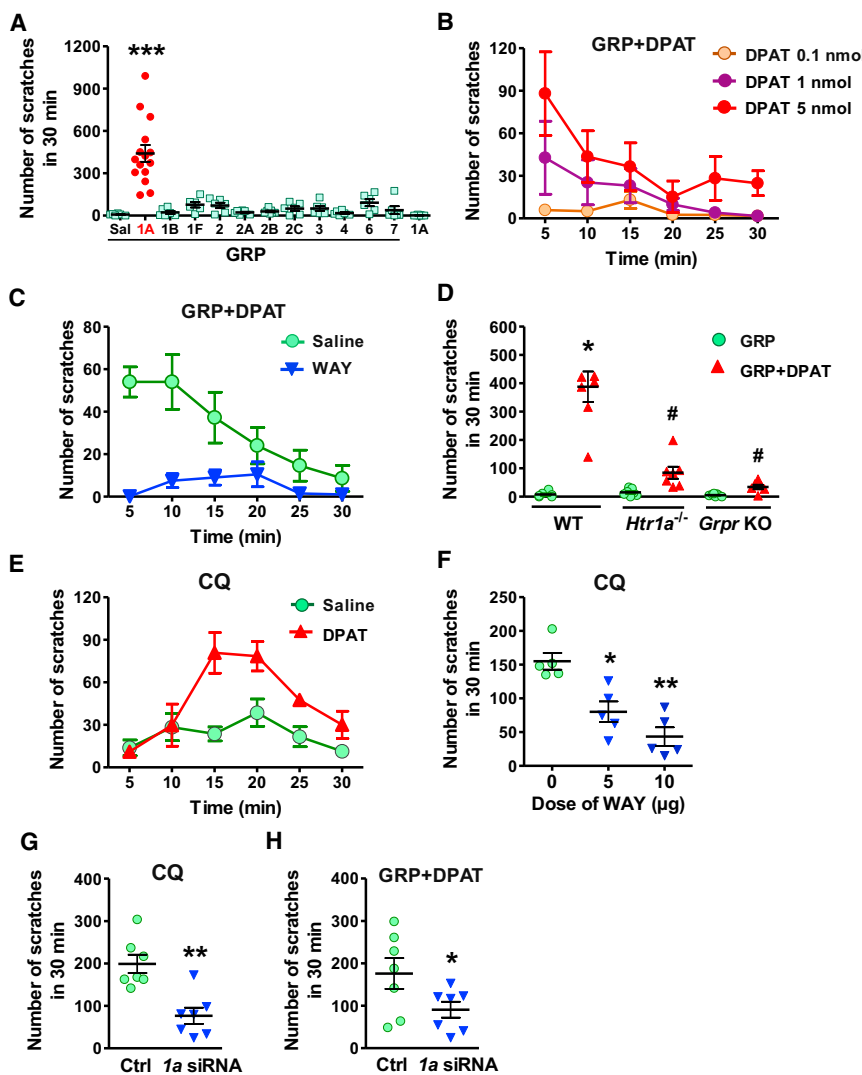


Figure 2. Serotonin Facilitates Scratching Behavior through 5-HT1A

(A) Scratching behaviors evoked by coinjection of GRP and various 5-HT receptor agonists (5 nmol) in WT mice. Sal, saline; 1A, DPAT; 1B, CP 93129; 1F, LY344864; 2, α -ME-5-HT; 2A, DOI; 2B, BW 723C86; 2C, m-cpp; 3, m-CPBG; 4, RS 67506; 6, EMD 386088; 7, AS-19.

(B) Coinjection of DPAT dose-dependently facilitated GIS ($p < 0.01$).

(C) WAY blocked the facilitatory effect of DPAT on GIS ($p < 0.01$).

(D) Coinjection of DPAT and GRP failed to elicit scratching behavior in *Htr1a*^{-/-} mice or *Grpr* KO mice.

(E–G) CQ-induced scratching behavior was significantly enhanced by DPAT ($p < 0.01$) (E), while attenuated by WAY (F) and *Htr1a* siRNA (1a siRNA) (G). (H) Facilitatory effect of DPAT on GIS was significantly reduced by *Htr1a* siRNA.

Error bars represent SEM ($n = 5-9$). * $p < 0.05$, ** $p < 0.01$, *** $p < 0.001$ versus saline (A, D, and F) or control (G and H). # $p < 0.05$ versus DPAT in WT. One-way ANOVA followed by Dunnett's multiple comparison test in (A), (D), and (F); two-way repeated-measures ANOVA in (B), (C), and (E); unpaired t test in (G) and (H).

WAY100635 (WAY), a highly specific 5-HT1A antagonist, to verify whether the robust scratching response elicited by DPAT/GRP is mediated by 5-HT1A. Pretreatment of mice with WAY (10 μ g, i.t.) for 5 min nearly abolished scratching behavior evoked by DPAT/GRP coinjection (Figure 2C). Importantly, DPAT failed to enhance scratching behavior in *Htr1a*^{-/-} mice and *Grpr* KO mice (Figure 2D). These data demonstrate that

activation of spinal 5-HT1A is required for the facilitation of GRPR function in itch transmission.

Since an elevated 5-HT level facilitates itch elicited by CQ, it is likely that 5-HT1A activation may facilitate CQ-elicited itch as well. Indeed, CQ-induced scratching behavior was greatly enhanced by i.t. DPAT (Figure 2E), mimicking the effect of 5-HTP (Figure 1H). Conversely, preinjection of WAY markedly attenuated CQ-induced scratching behavior (Figure 2F). Furthermore, CQ-induced scratching behavior was significantly attenuated after spinal siRNA knockdown of *Htr1a* (Figure 2G), which was functionally confirmed by reduced facilitatory effect of DPAT on GIS (Figure 2H). These results suggest that activation of spinal 5-HT1A is important for mediating descending 5-HT signaling to facilitate the function of GRPR in pruriceptive transmission.

Descending 5-HT Terminals Contact GRPR⁺ Neurons and Coexpression of 5-HT1A and GRPR in the Spinal Cord

5-HT terminals mainly originated from the NRM are densely distributed in the superficial part (laminae I and IIo) of the dorsal

5-HT1A Mediates 5-HT-Dependent Facilitation of GRPR Function

To identify the 5-HT receptor subtype that mediates the facilitating effect of descending 5-HT on itch transmission, we carried out pharmacological and behavioral screening by injecting a variety of 5-HT receptor agonists and GRP into the spinal cord of WT mice. GRP at 0.01 nmol was used because this dose was insufficient to elicit scratching behavior greater than vehicle (Figure 2A). The use of a minimal concentration of GRP serves to enhance the sensitivity of screening for identifying 5-HT receptor agonists that may potentiate GRP action. Of all the agonists tested for the 5-HT receptor subtypes, only R-(+)-8-OH-DPAT (DPAT), a 5-HT1A agonist, showed a robust facilitating effect on GIS (Figure 2A), and the effect of DPAT is dose dependent (Figure 2B). Notably, i.t. DPAT alone failed to induce scratch behavior (Figure 2A). Although DPAT is also a partial agonist for 5-HT7 receptor, it is unlikely that 5-HT7 is involved since AS-19, an agonist for 5-HT7, did not enhance GIS significantly (Figure 2A). Furthermore, agonists for other 5-HT receptor subtypes failed to increase GIS (Figure 2A). We next employed

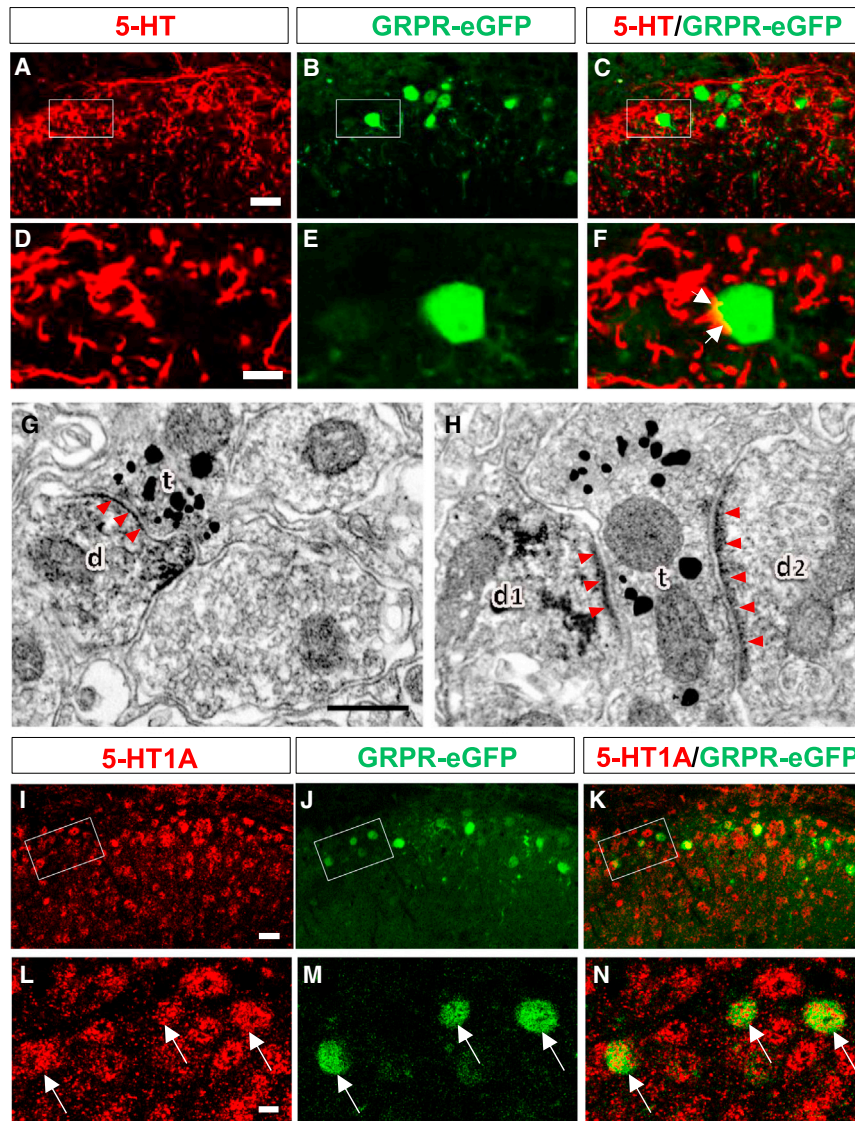


Figure 3. Coexpression of GRPR and 5-HT or 5-HT1A in the Spinal Cord

(A–F) Double IHC of 5-HT (red) and GFP (green) in the spinal cord of GRPR-eGFP mice show distribution of 5-HT⁺ terminals (A) and GRPR⁺ neurons (B) in the superficial dorsal horn. (C) An overlaid image of (A) and (B). (D) High-power image of the boxed area in (A). (E) High-power image of the boxed area in (B). (F) High-power image of the boxed area in (C). Arrows indicate close contacts between 5-HT⁺ terminals and GRPR⁺ neuronal cell bodies.

(G and H) 5-HT⁺ axon terminals (t; silver grains) make symmetric (G) or asymmetric (H) synaptic contacts with GRPR⁺ dendritic profiles (d, d1; DAB reaction products) or GRPR⁺ dendritic profile (d2), respectively. Arrow heads indicate postsynaptic membranes.

(I–N) Double IHC of 5-HT1A (red) and GFP (green) shows coexpression of 5-HT1A (I) and GRPR (J) in the superficial dorsal horn neurons. (K) An overlaid image of (I) and (J). (L) High-power image of the boxed area in (I). (M) High-power image of the boxed area in (J). (N) High-power image of the boxed area in (K). Arrows indicate double-stained cells.

Scale bars, 10 μ m in (A) and (I), 2.5 μ m in (D) and (L), 0.3 μ m in (G) and (H). See also [Figures S2](#) and [S3](#).

metric ones ([Figure 3H](#)). Therefore, serotonergic descending terminals predominantly make symmetrical synapses with GRPR⁺ neurons in the dorsal spinal cord.

One prerequisite for 5-HT1A and GRPR crosstalk is the coexpression of two partner receptors in the same neurons ([Pin et al., 2007](#)). The expression of 5-HT1A is heavily concentrated in the dorsal horn of the spinal cord ([Zhang et al., 2002](#)). To examine whether 5-HT1A is also expressed in GRPR⁺ neurons, we

performed double IHC of 5-HT1A and GFP in the spinal cord of GRPR-eGFP mice using anti-GFP antibody and anti-5-HT1A antibody ([Figure S2](#)). 5-HT1A is broadly expressed in the dorsal horn ([Figures 3I–3N](#)). Double IHC revealed that the overwhelming majority (91%) of GFP-expressing cells in the dorsal spinal cord were costained with 5-HT1A ([Figure 3N](#)). Moreover, we examined the coexpression of *Htr1a* and *Grpr* in GRPR-eGFP neurons using single-cell RT-PCR ([Figure S3B](#)) and found *Htr1a* mRNA signals in 78% (7/9) of eGFP⁺ neurons ([Table S1](#)). Furthermore, all eGFP⁺ neurons expressed *Grpr* mRNA ([Table S1](#)), validating the usage of eGFP as a marker for GRPR expression in GRPR-eGFP mice.

spinal cord and SpVc of the brainstem ([Li et al., 1997](#)). To examine whether 5-HT⁺ terminals make connections with GRPR⁺ neurons in the dorsal spinal cord, we performed double immunohistochemistry IHC for 5-HT and eGFP in GRPR-eGFP mice. Indeed, numerous 5-HT⁺ fibers and GRPR⁺ neurons were detected in the superficial laminae of the dorsal spinal cord, and 5-HT⁺ fibers overlap with all GRPR⁺ neurons ([Figures 3A–3F](#)). Synaptic connections between 5-HT⁺ terminals and GRPR⁺ neurons were further examined by electron microscopy using a double-immunolabeling method ([Li et al., 1997](#)) for 5-HT and eGFP. In the lumbar cord, both 5-HT⁺ terminals identified by the nanogold-silver enhancement and eGFP (GRPR)⁺ neurons revealed by the immunoperoxidase products were observed to distribute in the same pattern as found by our double IHC ([Figures 3A–3F](#)). 5-HT⁺ terminals form synapses with GRPR⁺ dendritic profiles ([Figures 3G and 3H](#)). Of the synaptic types characterized ([Uchizono, 1965](#)), 85.5% (71/83) were symmetric synapses ([Figure 3G](#)), while 14.5% (12/83) were asym-

performed double IHC of 5-HT1A and GFP in the spinal cord of GRPR-eGFP mice using anti-GFP antibody and anti-5-HT1A antibody ([Figure S2](#)). 5-HT1A is broadly expressed in the dorsal horn ([Figures 3I–3N](#)). Double IHC revealed that the overwhelming majority (91%) of GFP-expressing cells in the dorsal spinal cord were costained with 5-HT1A ([Figure 3N](#)). Moreover, we examined the coexpression of *Htr1a* and *Grpr* in GRPR-eGFP neurons using single-cell RT-PCR ([Figure S3B](#)) and found *Htr1a* mRNA signals in 78% (7/9) of eGFP⁺ neurons ([Table S1](#)). Furthermore, all eGFP⁺ neurons expressed *Grpr* mRNA ([Table S1](#)), validating the usage of eGFP as a marker for GRPR expression in GRPR-eGFP mice.

Facilitation of GRP-Induced Calcium Signaling by 5-HT1A in Spinal GRPR⁺ Neurons

GRPR mediates itch sensation through the PLC β /IP3 pathway and intracellular Ca²⁺ release ([Liu et al., 2011](#)), whereas 5-HT1A signals predominantly through the G_i protein-coupled

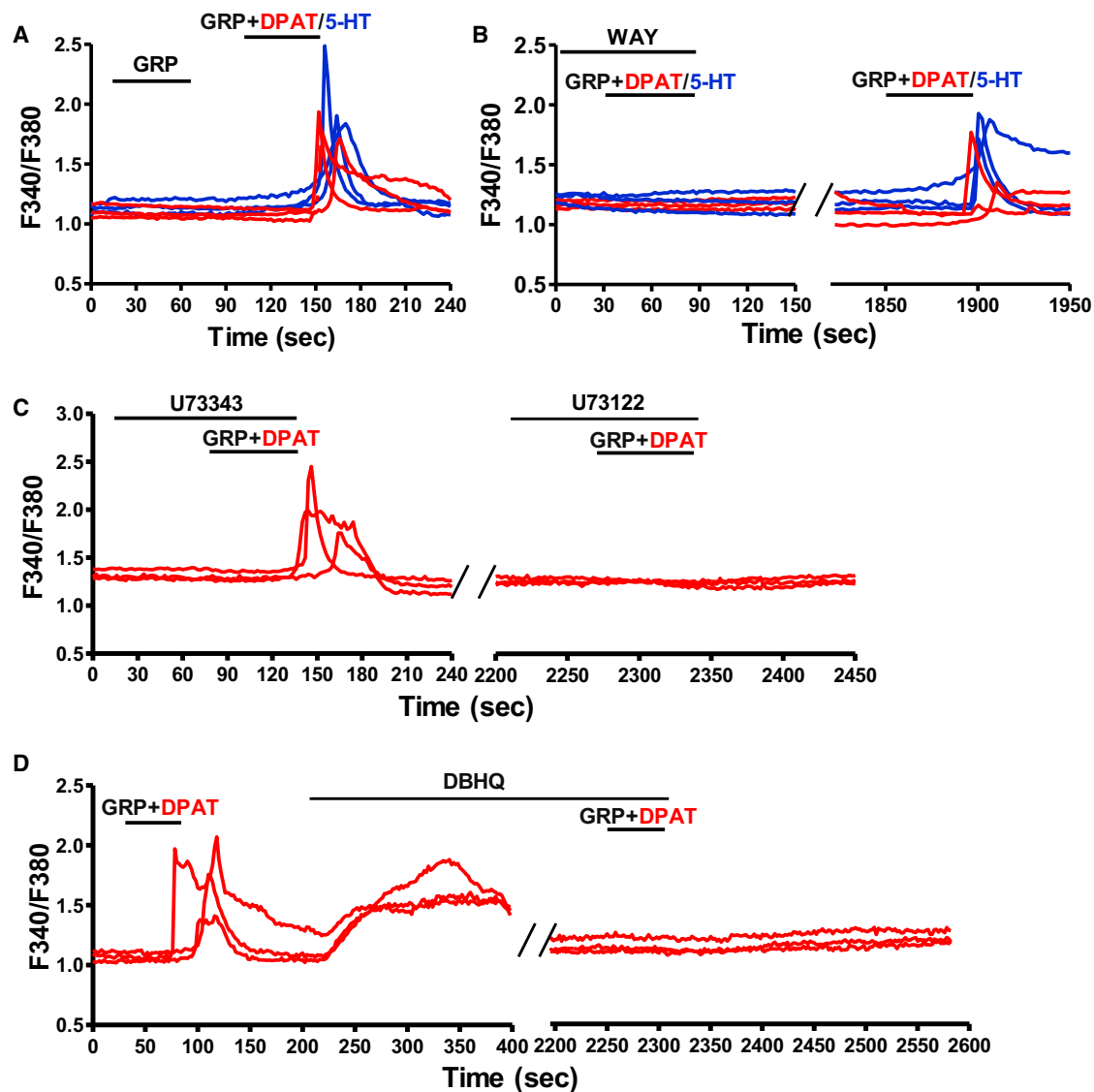


Figure 4. Coactivation of 5-HT1A Facilitates GRPR Ca^{2+} Signaling in Spinal Neurons

(A) Representative traces showing that 5 nM GRP failed to evoke Ca^{2+} responses in dissociated WT spinal neurons, while coapplication of 5-HT (blue) or DPAT (red) together with GRP (5 nM) induced intracellular Ca^{2+} mobilization. (B) WAY completely blocked Ca^{2+} responses of spinal neurons evoked by GRP+5-HT (blue) or GRP+DPAT (red), which recovered after WAY was washed out. (C) U73122, but not U73343, blocked intracellular Ca^{2+} mobilization induced by GRP+DPAT. (D) GRP+DPAT-evoked intracellular Ca^{2+} mobilization vanished after depletion of intracellular Ca^{2+} store by DBHQ. The experiments were repeated three times, and at least 200 neurons were analyzed for each experiment. See also [Figure S4](#).

cyclic AMP (cAMP) pathway (Hoyer et al., 2002). To investigate the functional cross-communication between 5-HT1A and GRPR, we examined intracellular Ca^{2+} mobilization in dissociated spinal dorsal horn neurons using calcium imaging. As expected, neither 5-HT nor DPAT at 10 μ M (Figure S4A), nor GRP at 5 nM, evoked a Ca^{2+} response in spinal dorsal horn neurons (Figure 4A). In contrast, coapplication of GRP (5 nM) and 5-HT (10 μ M) produced Ca^{2+} transients in 6% of spinal neurons (30/487) (Figure 4A), which cannot be attributed to additive effect. Similarly, DPAT (10 μ M) also greatly facilitated GRP-induced

Ca^{2+} signaling, indicating that 5-HT1A mediated the effect of 5-HT (Figure 4A). Importantly, spinal neurons of *Grpr* KO mice did not respond to GRP at high concentrations (up to 20 nM) (Figure S4B), indicating that it is GRPR that mediated the intracellular Ca^{2+} mobilization in WT neurons. To further examine the involvement of 5-HT1A in the observed facilitating effect of 5-HT and DPAT, WAY was used to block 5-HT1A prior to GRP+DPAT/5-HT application. Indeed, WAY completely blocked Ca^{2+} responses of GRPR⁺ neurons upon GRP+DPAT/5-HT incubation as well as the responses recovered after WAY was washed out

(Figure 4B). WAY did not display a nonspecific effect on intracellular Ca^{2+} mobilization evoked by GRP alone without 5-HT1A activation (Figure S4C). We previously showed that $G_q/PLC\beta/IP3R$ signaling pathway and intracellular Ca^{2+} stores are essential for GRP-induced Ca^{2+} response in human embryonic kidney 293 (HEK293) cells (Liu et al., 2011). To further understand the signaling events downstream of 5-HT1A/GRPR upon GRP+DPAT stimulation, we first tested the effect of U73122, a PLC inhibitor, and found that U73122, but not its inactive analog U73343, completely abolished GRP+DPAT-induced Ca^{2+} mobilization in GRPR⁺ neurons (Figure 4C). GRP+DPAT-responding neurons did not respond to the second incubation of GRP+DPAT after the intracellular Ca^{2+} store was depleted by 2,5-di-tert-butyl-hydroquinone (DBHQ), a selective and potent inhibitor of endoplasmic reticulum Ca^{2+} -ATPase (SERCA) (Moore et al., 1987) (Figure 4D). The effects of U73122 and DBHQ were not due to ligand-induced desensitization of 5-HT1A/GRPR signaling pathway because GRPR⁺ neurons showed comparable Ca^{2+} responses upon two consecutive applications of GRP+DPAT with a 30 min wash interval (Figure S4D). These results provide *in vivo* evidence indicating that coactivation of 5-HT1A by 5-HT or DPAT facilitates GRP/GRPR-mediated PLC-dependent intracellular Ca^{2+} signaling pathway.

Heteromeric Interactions between 5-HT1A and GRPR In Vitro and In Vivo

GPCR heteromeric interactions have been increasingly implicated in conferring GPCRs with expanded functionality (Bouvier, 2001; Milligan, 2013). Receptor crosstalk confers neuronal GPCRs with novel signaling and pharmacological properties enhancing the capacity of neural circuits to regulate a wide array of behavioral outputs (Prinster et al., 2005). The coexpression and synergistic effect of 5-HT1A and GRPR coactivation raised the possibility that these two receptors may function as receptor heteromeric complexes. To ascertain whether 5-HT1A and GRPR may physically interact through receptor heteromerization, we conducted coimmunoprecipitation (coIP) experiments using membrane proteins extracted from HEK293 cells coexpressing HA-5-HT1A and Myc-GRPR. Anti-Myc antibody coimmunoprecipitated a band that corresponds to HA-5-HT1A (Figure 5A). In a reverse coIP experiment, a specific Myc-GRPR band was also detected in anti-HA precipitates (Figure 5B). In contrast, the specific bands were not observed in the precipitates from mixed membrane proteins that were prepared using cells expressing either HA-5-HT1A or Myc-GRPR (Figures 5A and 5B), suggesting the presence of constitutive 5-HT1A-GRPR complexes in the membrane when these two receptors are coexpressed in the same cells (Figures 5A and 5B). To verify the specificity of coIP between HA-5-HT1A and Myc-GRPR, we examined whether GRPR would interact with 5-HT1B, a 5-HT1 receptor subtype that is phylogenetically most closely related to 5-HT1A (Hoyer et al., 2002). Myc-GRPR immunoreactivity was not detectable in HA-5-HT1B precipitates using HEK293 cells coexpressing HA-5-HT1B and Myc-GRPR (Figure 5C). These results suggest that the formation of 5-HT1A and GRPR heteromers is likely to be specific. Next, we examined whether 5-HT1A and GRPR interact with each other *in vivo* by coIP studies using the spinal cord membrane preparations (Liu

et al., 2011). A specific 5-HT1A band was coimmunoprecipitated with GRPR using mouse anti-GRPR antibodies (Figure 5D) but was not detectable when an irrelevant mouse immunoglobulin G (IgG) was used (Figure 5D). Taken together, these results suggest the presence of receptor heteromeric complexes containing 5-HT1A and GRPR both *in vitro* and *in vivo*. Moreover, it further confirms that the two receptors are coexpressed in the same neurons in the spinal cord.

5-HT1A and GRPR Are Located in Close Proximity

Although coIP data suggest a physical association between 5-HT1A and GRPR, it remained unclear whether the receptors themselves interact or if intermediaries such as scaffolding or anchoring proteins were required for receptor association or whether the two receptors may coexist in microdomains (Prezeau et al., 2010). To examine this possibility, we utilized confocal imaging and single-cell subcellular acceptor photobleaching fluorescence resonance energy transfer (FRET) analysis to assess the physical association between 5-HT1A and GRPR receptors (Karunarathne et al., 2013). A major advantage of our confocal setup is that the analysis of FRET can be performed in subcellular compartments on a single-cell level. This allows us to use a defined region of the same cell that is not photobleached as an internal control. The C terminus of 5-HT1A and GRPR were tagged with fluorescent protein eGFP as the donor and mCherry as the acceptor, respectively. FRET is calculated by time-lapse imaging of donor GFP (488 excitation, 510 emission) and acceptor mCherry (488 excitation, 630 emission) before and after photobleaching the acceptor (mCherry) in a selected region of the plasma membrane (Figure 5E). A plasma membrane region in the same cell that was not photobleached served as control (Figure 5E). Fast photobleaching (0.89 ms/ μm^2) and slow mobility of several transmembrane receptors on the plasma membrane ensured that during FRET analysis both the donor and acceptor fluorescent proteins remained stationary. After acceptor (5-HT1A-mCherry) photobleaching, donor (GRPR-eGFP) fluorescence intensity was increased due to the loss of energy transfer, suggesting the presence of FRET (Figures 5F and 5G). The FRET loss associated with acceptor photobleaching and subsequent increase in donor fluorescence intensity was $44.8\% \pm 11.2\%$ (Figures 5F and 5G). In contrast, no detectable FRET signal was observed between 5-HT1B-mCherry and GRPR-eGFP (Figure S6B). Lack of FRET between 5-HT1B and GRPR is consistent with coIP results, further supporting the notion that the 5-HT1A-GRPR association is specific. Taken together, these results suggest that 5-HT1A and GRPR are in close proximity on the plasma membrane, which may facilitate crosstalk between the two receptors.

Activation of 5-HT1A Potentiates the Excitability of GRPR⁺ Neurons

We next evaluated the effect of 5-HT1A activation on GRP-induced excitation of GRPR⁺ neurons by whole-cell patch-clamp recordings of GRPR-eGFP neurons using spinal cord slice preparations, hereafter referred to as GRPR⁺ neurons (Zhao et al., 2013). We first measured changes in membrane potential and input resistance of GRPR⁺ neurons in response to GRP, DPAT, and 5-HT. A bath application of GRP induced a subthreshold

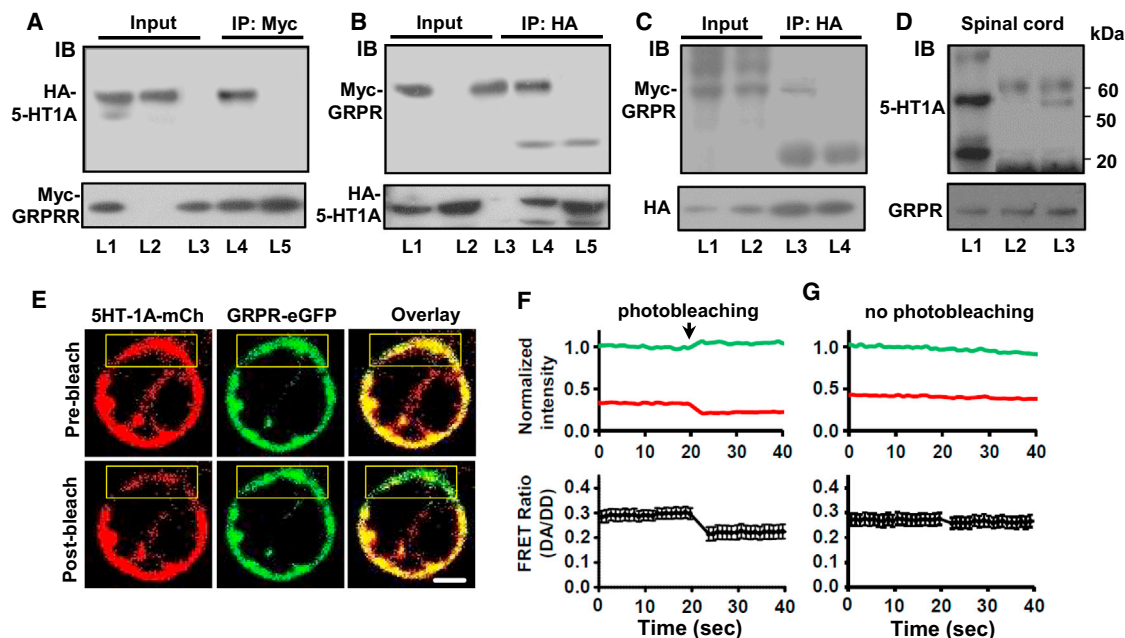


Figure 5. GRPR and 5-HT1A Form Heteromeric Complexes and Are within Close Proximity

(A and B) When coexpressed in same cells, immunoblotting (IB) bands corresponding to HA-5-HT1A and Myc-GRPR were both found in the precipitates of anti-Myc antibody (A) or anti-HA antibody (B). L1 and L4, HA-5-HT1A/Myc-GRPR cells; L2, HA-5-HT1A cells; L3, Myc-GRPR cells; L5, mixture of L2 and L3.

(C) Myc-GRPR was not coimmunoprecipitated with HA-5-HT1B. L1, L3, HA-5-HT1A/Myc-GRPR cells; L2, L4, HA-5-HT1B/Myc-GRPR cells.

(D) CoIP of 5-HT1A and GRPR from the spinal cord membrane preparations. L1, input; L2, irrelevant mouse IgG; L3, mouse anti-GRPR.

(E) Representative confocal images show one HEK293 cell coexpressing 5HT1A-mCherry (red) and GRPR-eGFP (green), before and after acceptor (mCherry) photobleaching in selected regions of the cell (yellow box). Scale bar, 10 μ m.

(F) Top: plots showing background subtracted normalized fluorescence intensities of donor emission (green trace, 488 nm excitation, 515 nm emission: DD) and acceptor emission (red trace, 488 nm excitation, 630 nm emission: DA) from selected plasma membrane regions in (E). Bottom: averaged FRET ratio (DA/DD) of the photobleached regions in (E).

(G) Background subtracted normalized fluorescence intensities (top) and averaged FRET ratio (bottom) of nonphotobleached plasma membrane regions in (E). Number of cells, $n = 9-11$. Error bars represent SEM. See also [Figures S5](#) and [S6](#).

membrane depolarization ([Figures 6A](#) and [6E](#)). In contrast, DPAT and 5-HT hyperpolarized GRPR⁺ neurons as expected ([Figures 6B](#), [6C](#), and [6E](#)). Thus, activation of GRPR and 5-HT1A alone appeared to have opposing effects on the excitability of GRPR⁺ neurons in the spinal cord. To determine whether DPAT or 5-HT could facilitate GRP-dependent excitation, we examined the effect of a coapplication of GRP and DPAT or 5-HT on GRPR⁺ neurons. Importantly, a coapplication of GRP+DPAT or GRP+5-HT not only masked the hyperpolarization observed in response to DPAT or 5-HT alone, but also induced a larger magnitude of depolarization that often resulted in action potential (AP) firing ([Figure 6D](#)). GRP and GRP+DPAT treatments significantly increased input resistance compared to control, whereas DPAT alone significantly decreased input resistance compared to control ([Figures 6F](#) and [6G](#)). These data revealed that GRP-induced subthreshold membrane depolarization not only counteracted the hyperpolarizing effect of DPAT but was also potentiated by DPAT with a net increase in the excitability of GRPR⁺ neurons.

A Blockade of 5-HT1A Attenuates Chronic Itch

In light of the facilitatory effect of 5-HT1A on GRPR signaling and CQ-elicited itch, we next asked whether 5-HT1A could modulate

long-lasting scratching behavior using two distinct chronic itch models that are dependent on enhanced GRP/GRPR signaling for maintaining long-lasting itch transmission ([Zhao et al., 2013](#)). First, we tested the effect of 5-HT1A activation on spontaneous scratching behavior of BRAF^{Nav1.8} mice in which the BRAF kinase in sensory neurons expressing the sodium channel Nav1.8 was selectively activated by genetically replacing the WT *Braf* gene with a kinase-activated one (V600E) ([Zhao et al., 2013](#)). BRAF^{Nav1.8} mice progressively developed spontaneous scratching behavior accompanied by skin lesions as a result from increased expression of a cohort of itch-related genes, including GRP in sensory neurons and GRPR in the spinal cord ([Zhao et al., 2013](#)). Although WT mice failed to exhibit scratching behavior after i.t. DPAT alone, the spontaneous scratching behavior of BRAF^{Nav1.8} mice was significantly enhanced ([Figure 7A](#)). Likewise, DPAT also significantly enhanced the chronic scratching behavior induced by dry skin (xerosis) ([Figure 7B](#)), a skin condition often associated with pruritus ([Miyamoto et al., 2002](#)). The enhanced scratching responses in mice with chronic itch by DPAT suggests that 5-HT1A is likely to be constitutively primed for tonic activation by enhanced release of 5-HT. To test this, we measured the levels of 5-HT and 5-HIAA in mice with chronic itch using HPLC. Moreover, the levels of 5-HT

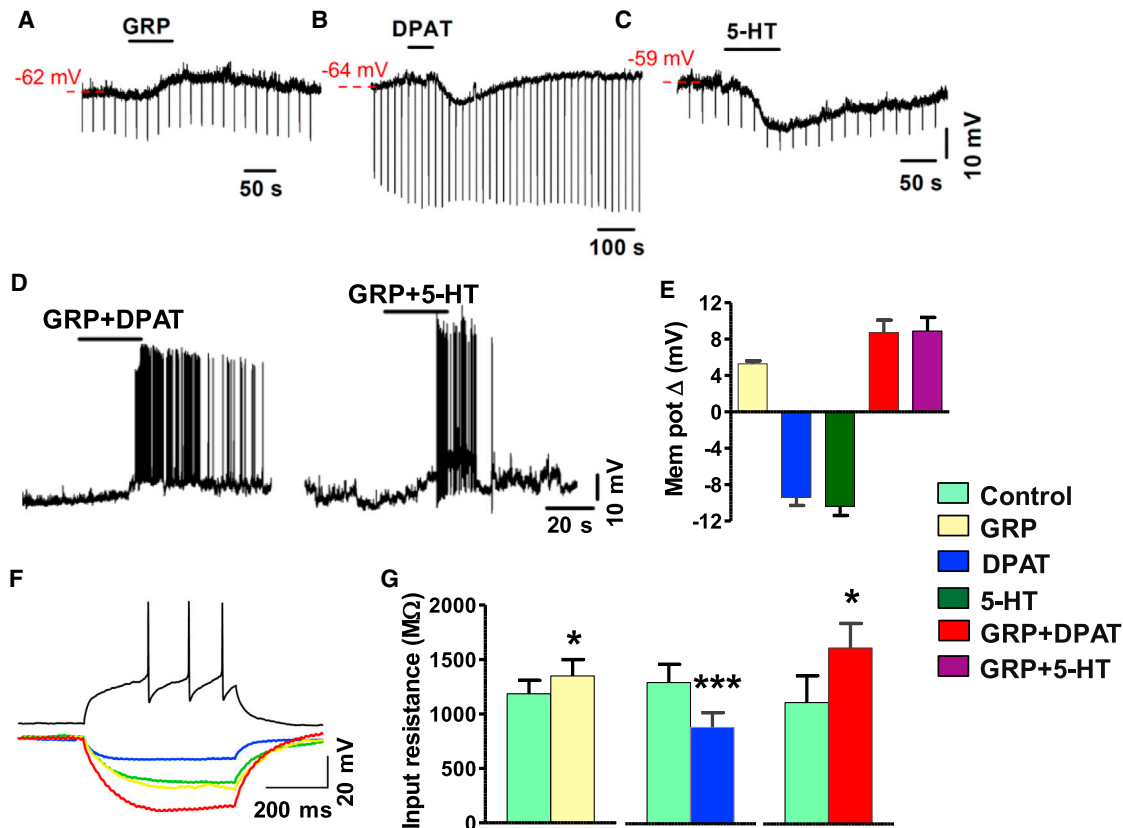


Figure 6. Coactivation of 5-HT1A and GRPR Increases the Excitability of GRPR⁺ Neurons

(A–C) Representative traces show membrane depolarization by GRP (A) and hyperpolarizing response induced by DPAT (B) and 5-HT (C) in current-clamped GRPR⁺ neurons.

(D) Representative traces showing that a coapplication of GRP and DPAT or 5-HT evoked membrane depolarization and AP firing in current-clamped GRPR⁺ neurons. AP firing evoked by GRP+DPAT and GRP+5-HT ranged from 0.167 to 3.5 Hz (n = 6) and 0.03 to 6 Hz (n = 17), respectively.

(E) Quantified data of (A)–(D). GRP depolarized GRPR⁺ neurons by 5.3 ± 0.3 mV (n = 8). DPAT (7.5 μM, blue) and 5-HT (40 μM, dark green) hyperpolarized GRPR⁺ neurons by 9.4 ± 0.9 mV (n = 19) and 10.4 ± 1 mV (n = 13), respectively. In contrast, coapplication of GRP+DPAT depolarized GRPR⁺ neurons by 8.7 ± 1.4 mV (red) (n = 15). GRP+5-HT depolarized GRPR⁺ neurons by 8.9 ± 1.5 mV (purple) (n = 35).

(F) Representative traces illustrate the effect of GRP (yellow), DPAT (blue), and GRP+DPAT (red) on membrane input resistance in current-clamped GRPR⁺ neurons receiving negative current injections (–20 pA). Control (green): extracellular buffer only. For all recordings, neuronal health was verified by observing action potentials in response to positive current injection under control conditions (black).

(G) GRP (yellow) increased the membrane input resistance from $1,185 \pm 124$ MΩ to $1,350 \pm 150$ MΩ (n = 8), DPAT decreased the input resistance from $1,311 \pm 168$ MΩ to 894 ± 137 MΩ (n = 19), and GRP + DPAT increased the input resistance from $1,116 \pm 247$ MΩ to $1,616 \pm 226$ MΩ (n = 15); *p < 0.05, **p < 0.01, ***p < 0.001, paired t test.

Error bars represent SEM.

were significantly elevated in the hindbrain of BRAF^{Nav1.8} mice and cervical spinal cord of dry skin mice (Figure S7A). The levels of 5-HIAA were also significantly elevated in hindbrain and cervical spinal cord of BRAF^{Nav1.8} mice, suggesting enhanced activity of 5-HT in these regions (Figure S7B). Then, we examined whether WAY may attenuate chronic itch. Similar to its inhibitory effect on CQ-elicited itch, i.t. WAY significantly attenuated spontaneous scratching behaviors of BRAF^{Nav1.8} mice (Figure 7C) and dry skin mice (Figure 7D). Importantly, injection of saline had no significant effect on spontaneous scratching behaviors of BRAF^{Nav1.8} mice or dry skin mice (Figures 7C and 7D). Furthermore, *Tph2*^{-/-} mice also displayed deficits in spontaneous scratching behaviors under dry skin condition (Figure 7E), and WT mice showed attenuated scratching behavior after knock-

down of spinal 5-HT1A by i.t. *Htr1a* siRNA (Figure 7F). Thus, these data support the notion that 5-HT1A is constitutively activated in the setting of chronic itch, and its activation by descending 5-HT is required for maintaining long-lasting itch transmission.

DISCUSSION

The Role of 5-HT1A in the Modulation of Itch Transmission

Using both loss- and gain-of-function, genetic, pharmacological, behavioral, and electrophysiological examinations, we demonstrate that central 5-HT signaling is essential for facilitating itch transmission, and this function is mediated by the 5-HT1A

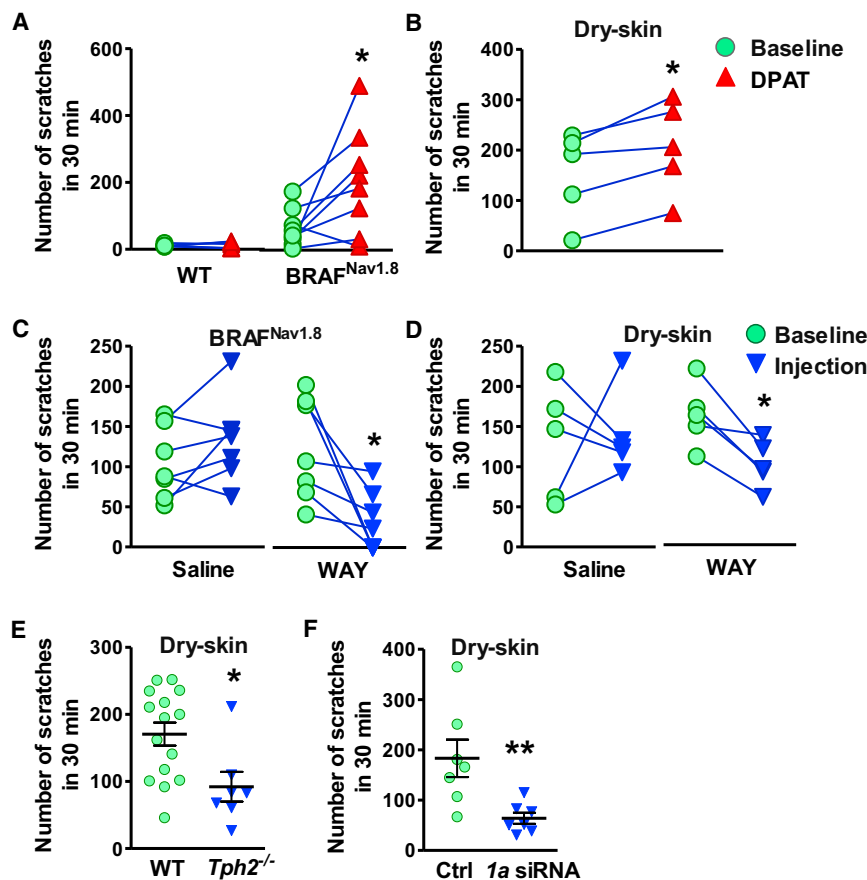


Figure 7. Activation of 5-HT1A Facilitates Long-Lasting Itch Transmission

(A and B) Spontaneous scratching behaviors of BRAF^{Nav1.8} mice (A) and dry skin mice (B) were facilitated after DPAT injection.

(C and D) WAY (10 μg) suppressed spontaneous scratching behavior of BRAF^{Nav1.8} mice (C) and dry skin mice (D).

(E) *Tph2*^{-/-} mice showed attenuated spontaneous scratching behavior under dry skin condition compared to WT littermates.

(F) *Htr1a* siRNA treatment significantly attenuated spontaneous scratching behavior under dry skin condition compared to control siRNA (Ctrl).

Error bars represent SEM (n = 5–15). *p < 0.05, paired t test in (A)–(D), unpaired t test in (E) and (F). See also Figure S7.

receptor. Decreased itch transmission in mice lacking 5-HT is unlikely to be due to developmental deficits because we were able to restore normal itch transmission in *Tph2*^{-/-} mice by an administration of exogenous 5-HTP. Furthermore, we demonstrate that central 5-HT neurons are essential for converting 5-HTP into 5-HT since mice lacking these neurons failed to be rescued by exogenous 5-HTP. Our study reveals a function of 5-HT in sensory modality-specific modulation and demonstrate that 5-HT1A is a principal receptor for mediating 5-HT-dependent modulation of itch transmission. Importantly, the facilitatory role of 5-HT1A is required not only for acute itch but also for long-lasting itch transmission. Therefore, 5-HT1A has a broad role in the modulation of itch transmission.

5-HT1A-GRPR Crosstalk Amplifies Itch Signaling

A key finding of our work is that 5-HT1A facilitates itch modulation through its crosstalk with GRPR. Several pieces of evidence, such as coexpression, colP, and FRET data, imply a physical association between 5-HT1A and GRPR in the same cells. While further studies are needed to explain whether the existence of 5-HT1A-GRPR heteromeric complexes is a prerequisite for the initiation of signaling crosstalk, it is tempting to speculate that the spatial proximity of 5-HT1A and GRPR may permit specific heteromeric crosstalk without accidental engagement of unrelated signaling pathways in GRPR⁺ neurons. A close proximity with 5-HT1A may enable GRPR to process information via pairing

with specific GPCRs in a real-time manner. 5-HT1A-dependent facilitation requires coactivation of GRPR by exogenous GRP. Although coapplication of GRP is not required in chronic itch models for 5-HT1A-dependent facilitation, it is presumed that there is a constitutive release of GRP from primary afferents to prime GRPR for 5-HT modulation because GRP expression is significantly upregulated in chronic itch conditions and GRP blocker attenuated spontaneous scratching behaviors (Liu et al., 2014; Nattkemper et al., 2013; Zhao et al., 2013).

The mode of 5-HT1A or GRPR activation in a single-receptor paradigm clearly differs from that of the two-receptor paradigm. The fact that DPAT by itself is unable to elicit scratching behavior implies that 5-HT1A cannot transmit itch information directly. In contrast, GRP at a low dose that is insufficient to elicit either a calcium response (5 nM) or scratching behavior (0.01 nmol) can do so only if 5-HT1A is simultaneously activated. Since DPAT alone fails to produce calcium spikes, it is unlikely that DPAT alone is capable of exciting GRPR⁺ neurons. On the contrary, DPAT causes hyperpolarization of GRPR⁺ neurons. Postsynaptic 5-HT1A activation predominantly hyperpolarizes dorsal horn neurons to dampen neuronal excitability and synaptic transmission (Grudt et al., 1995; Yoshimura and Furue, 2006). Remarkably, the hyperpolarizing response of GRPR⁺ neurons produced by DPAT was completely masked by GRP. When GRP and DPAT were coapplied, together they were able to induce action potential firing. This response was not observed by an application of either GRP or DPAT alone. Thus, interactions between 5-HT1A and GRPR alter the pharmacological and physiological properties of either of the receptors and confer a unique functionality to 5-HT1A (Figure 8A). While activation of G_i-coupled 5-HT1A is usually inhibitory via the cAMP pathway, the receptor may facilitate the responsiveness of G_q-coupled receptors through signaling coupling. Our finding thus uncovers a unique paradigm for exploring facilitatory crosstalk mechanisms between G_i- and G_q-coupled receptor signaling transduction in a highly

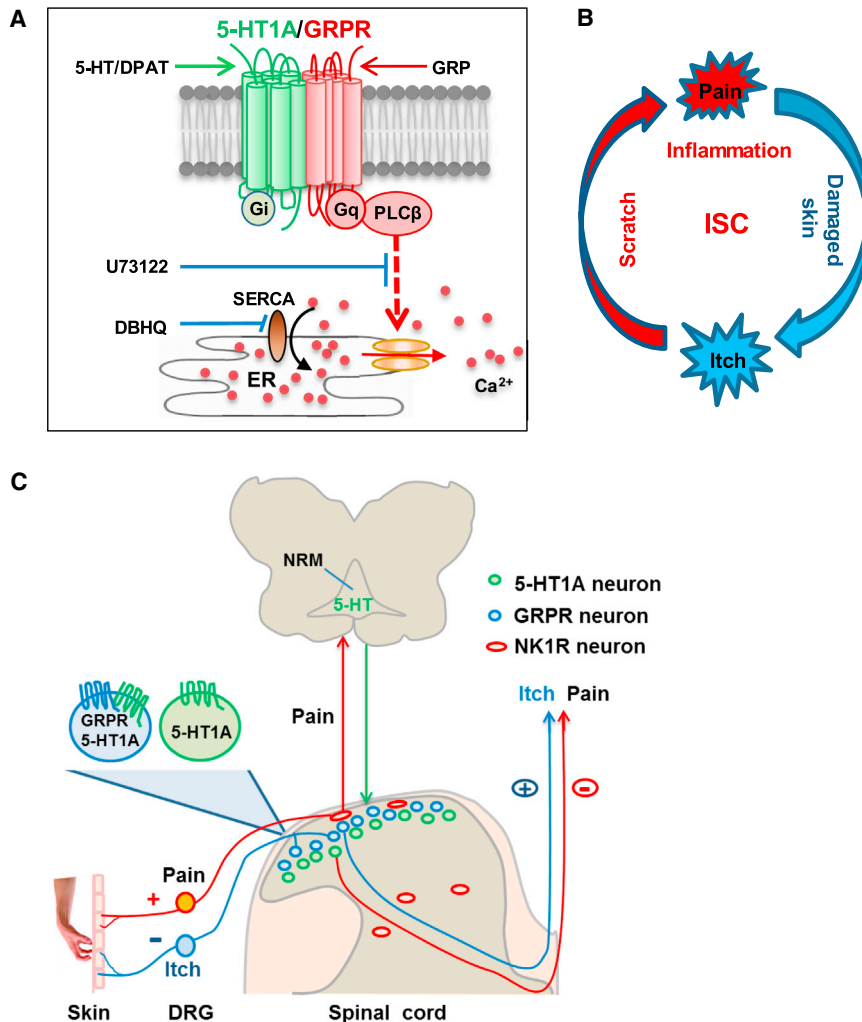


Figure 8. Hypothetic Models Illustrating the Role of 5-HT/5-HT1A in the Itch-Scratch Cycle

(A) Schematic showing signaling interactions between 5-HT1A and GRPR. Coactivation of 5-HT1A and GRPR amplifies G_q -coupled $PLC\beta$ -dependent signaling pathway, resulting in the release of Ca^{2+} from ER through SERCA pumps. ER: endoplasmic reticulum.

(B) Schematic that illustrates the vicious ISC. Scratching induces skin inflammation, which in turn induces more vicious itching attacks.

(C) Schematic of dual modulation of descending 5-HT signaling in pain and itch during the ISC. Scratching evokes inflammatory/mechanical pain, which results in the activation of 5-HT neurons in NRM of the brainstem. Descending release of 5-HT acts on two distinct subpopulations of neurons: one expressing 5-HT1A alone (green cells) that inhibits nociceptive processing and the other expressing both 5-HT1A and GRPR (blue cells) that facilitates pruriceptive transmission. NRM: nucleus raphe magnus.

ably, may be subject to opposing descending modulation in the spinal cord. Despite some conflicting reports and the pain modality-dependent role of 5-HT1A (Bardin, 2011), most studies suggest an inhibitory function for postsynaptic 5-HT1A in spinal nociceptive processing, especially in thermal and inflammatory pain (Bardin, 2011; Millan, 2002; Yoshimura and Furue, 2006; Zhao et al., 2007a). The majority of substantia gelatinosa (lamina II) neurons of the dorsal horn and SpVc responded to 5-HT or 5-HT1A agonists with a hyperpolarizing

physiologically relevant context. It is important to note that the present study is only one step toward understanding the central modulation of itch transmission. Since both heteromeric interactions and/or convergence of intracellular signaling pathways may occur (Prezeau et al., 2010), our studies raise several key questions concerning the underlying mechanisms: what are the interfacing regions for 5-HT1A-GRPR heteromeric interaction? Does the crosstalk between 5-HT1A and GRPR occur at the receptor or intracellular second messenger levels or both? If intracellular crosstalk is required, does 5-HT1A potentiate GRPR signaling by releasing $G_{\beta\gamma}$ subunits to stimulate G_q -coupled PLC signaling? What is the respective role of G_i -coupled signaling in activation versus facilitation of GRPR? It will be of great interest to determine where the two signaling pathways might converge to amplify G_q -dependent itch signaling through either a “switch” or “turn off” of the signaling characteristic of G_i -coupled receptors.

Opposing Modulation of Itch and Pain by 5-HT Receptor Mechanisms

Pain and itch have been known as two opposing sensations (Ikoma et al., 2006; LaMotte et al., 2014; Ma, 2010) and, conceiv-

ably, may be subject to opposing descending modulation in the spinal cord. Despite some conflicting reports and the pain modality-dependent role of 5-HT1A (Bardin, 2011), most studies suggest an inhibitory function for postsynaptic 5-HT1A in spinal nociceptive processing, especially in thermal and inflammatory pain (Bardin, 2011; Millan, 2002; Yoshimura and Furue, 2006; Zhao et al., 2007a). The majority of substantia gelatinosa (lamina II) neurons of the dorsal horn and SpVc responded to 5-HT or 5-HT1A agonists with a hyperpolarizing membrane current, thereby inhibiting nociceptive processing (Abe et al., 2009; Grudt et al., 1995; Lu and Perl, 2007; Yoshimura and Furue, 2006). In contrast, 5-HT1A facilitates itch by enhancing the excitability of GRPR⁺ neurons and by inhibiting its canonical pathway. Taken together, 5-HT1A has opposing roles in mediating descending 5-HT modulation of itch and pain, and this dual role is exerted through distinct subsets of dorsal horn neurons that express 5-HT1A with or without GRPR (Figure 8C). Along with previous studies, our data therefore provide evidence indicating that itch and pain are subject to opposing modulation of descending 5-HT signaling in the spinal cord.

Contribution of Central 5-HT Signaling to Development of the Itch-Scratch Cycle

What is the probable physiological significance of 5-HT1A-mediated central modulation of itch and pain? A cardinal feature of chronic itch associated with a wide spectrum of skin diseases is a vicious itch-scratch cycle (ISC) (Paus et al., 2006; Yosipovitch and Papoiu, 2008) (Figure 8B). Scratching behavior, as a noxious mechanical stimulus, can inhibit itch sensation and spinal projection neurons (Davidson et al., 2009; Yosipovitch et al.,

2007). However, it also intensifies skin inflammation, which in turn provokes more intense itch sensation as well as an uncontrollable urge to scratch. Given the role of postsynaptic 5-HT1A in the inhibition of inflammatory pain and spinal nociceptive processing, we suggest a hypothetic model that explains the dual consequences of scratching behavior (Figure 8C). Past studies indicated that activation of the nociceptive pathway in response to somatic and/or noxious stimuli can promote 5-HT release in the spinal cord (Sorkin and McAdoo, 1993; Yaksh and Tyce, 1981). Likewise, vigorous scratching-induced pain can conceivably evoke 5-HT release to inhibit nociceptive processing through 5-HT1A-dependent negative feedback mechanisms (Figure 8B). Concurrently, tonic 5-HT release paradoxically activates 5-HT1A in GRPR⁺ neurons to potentiate itch transmission (Figure 8C). Thus, the positive and negative feedback controls of pain and itch outputs are likely to contribute to the vicious development of the ISC.

Because cross-signaling of 5-HT1A-GRPR heteromers is itch specific (only when GRPR is activated), a disruption of an interface between 5-HT1A and GRPR may alleviate the urge to scratch in chronic itch conditions. The advantage of such a strategy is to permit the normal functioning of 5-HT1A and GRPR in other areas of the brain where the receptors are not coexpressed. Unraveling key interfaces required for 5-HT1A-GRPR cross-signaling could be a crucial next step. Since GPCR crosstalk may occur at multiple signaling levels, the converging points of G_i-G_q cross-signaling may also be substrates for a therapeutic blockade. As enhanced central 5-HT signaling is likely to exacerbate the ISC, an exploration of the disruption of modulatory function of 5-HT1A opens an additional avenue for designing novel therapeutics that ameliorate chronic pruritus.

EXPERIMENTAL PROCEDURES

Animal Behavior

Adult male C57BL/6J mice, *Lmx1b*^{fl/fl} mice (Zhao et al., 2006), *Tph2*^{-/-} mice (Kim et al., 2014), *Htr1a*^{-/-} mice (Heisler et al., 1998), *Grpr* KO mice (Hampton et al., 1998), and BRAF^{Nav1.8} mice (Zhao et al., 2013) were used for the study. Scratching behaviors were performed as previously described (Sun and Chen, 2007; Zhao et al., 2013). All animal experiments were performed in accordance with the guidelines of the National Institutes of Health and the International Association for the Study of Pain and were approved by the Animal Studies Committee at Washington University School of Medicine.

Immunohistochemistry and In Situ Hybridization

IHC and ISH were performed as described (Zhao et al., 2006). For the IHC study, sections were incubated with primary antibodies overnight at 4°C followed by the use of FITC or Cy3-conjugated secondary antibodies (Jackson ImmunoResearch). The following primary antibodies were used: rabbit anti-5-HT (1:5,000, Immunostar), rabbit anti-5-HT-1A (1:200, Santa Cruz), and chicken anti-GFP (polyclonal, 1:500, Aves Labs). For the ISH study, a digoxigenin-labeled cRNA probe was used as described earlier (Zhao et al., 2006). Images were taken using a Nikon Eclipse Ti-U microscope.

Small Interfering RNA Treatment

Htr1a siRNA (Sigma) were delivered to the lumbar region of the spinal cord twice daily for six consecutive days as described previously (Liu et al., 2011). Behavioral testing was carried out 24 hr after the last injection.

Immune-Electron Microscopy

Immune-electron microscopic studies were performed as described (Li et al., 1997; Pang et al., 2006). Briefly, cross sections of lumbar spinal cord of adult

GRPR-eGFP mice were double immune-labeled by rabbit anti-5-HT antibody (1:2,000; Incstar Corporation) and guinea pig anti-GFP antibody (1.5 μg/ml) using immunogold-silver and immunoperoxidase methods, respectively. Furthermore, 50 nm-thick ultrathin sections were examined with a JEM-1400 electron microscope (JEM). The digital micrographs were captured by VELETA (Olympus).

HPLC

The concentrations of monoamines were measured as previously described (Zhao et al., 2006). The resulting values were corrected for volume and expressed as pg of amine per mg of wet tissue or per 100 μl of plasma. For analyzing the effect of 5-HTP injections on indoleamine concentrations, samples were collected 1 hr after 5-HTP or saline administration.

Cell Culture and Transfections

Constructs were transfected into HEK293 cell lines for selection as described (Liu et al., 2011). For FRET experiments, pcDNA3.1/GRPR-eGFP (1 μg/cm²) and pcDNA3.1/5-HT1A-mCherry (0.2 μg/cm²) were transiently transfected into HEK293 cells using Lipofectamine 2000 (Invitrogen). FRET was done 24 hr after transfection.

Calcium Imaging, CoIP, and Western Blot Analysis

Calcium imaging experiments were performed as described previously (Liu et al., 2011). Experiments were repeated three times, and a minimum of 50 cells were included for analysis. CoIP and western blot analysis were performed as described (Liu et al., 2011). Briefly, solubilized membrane proteins (200 μg) were precipitated with rabbit anti-HA (BD Bioscience), mouse anti-Myc (Covance), or mouse anti-GRPR (Abmart) antibodies and TrueBlot anti-rabbit or anti-mouse IgG bead slurry (eBioscience). After elution, proteins were analyzed using western blot with mouse anti-Myc (1:1,000), rabbit anti-HA (1:1,000), mouse anti-GRPR (1:5,000), or rabbit anti-5-HT1A (1:5,000, Abcam).

Confocal Subcellular FRET Imaging

The FRET imaging and calculations were performed as described previously (Karunarathne et al., 2013). Basal FRET between eGFP (donor) and mCherry (acceptor) was measured by rapid photobleaching of the acceptor in a defined region of a single cell, whereas the unbleached region was used as the control. Before and after photobleaching, a series of time-lapse images were captured with donor excitation-donor emission (DD) and donor excitation-acceptor emission (DA).

Electrophysiological Recording

Patch-clamp studies were performed as described previously (Jeffry et al., 2009). Slices of the lumbar spinal cord of GRPR-eGFP mice 3–4 weeks of age were prepared for patch-clamp recording. Firing patterns were examined by injection of steps of positive current for 500 ms. Input resistance was tested every 20 s for drug-induced changes by an injection of negative current (−20 pA). Series resistance was monitored in voltage clamp mode by measuring the instantaneous current in response to small voltage steps. Data were analyzed offline (ClampFit 10) and plotted in Origin 8 graphing software.

Statistical Analysis

Statistical analyses were performed using Prism 5 (version 5.03, GraphPad Software). $p < 0.05$ was considered statistically significant.

SUPPLEMENTAL INFORMATION

Supplemental Information includes Supplemental Experimental Procedures, seven figures, and one table and can be found with this article online at <http://dx.doi.org/10.1016/j.neuron.2014.10.003>.

AUTHOR CONTRIBUTIONS

Z.-Q.Z., X.-Y.L., L.W., Y.-G.S., and P.M. performed pharmacological and behavioral experiments; X.-Y.L. performed coIP experiment; and J.J.

performed electrophysiological recording. W.K.A.K. and A.M. performed FRET analysis. J.-L.L. and Z.-Y.W. performed EM experiment. X.-Y.Z. performed Ca^{2+} imaging; H.L., Z.-Y.W., F.-Q.H., D.M.B., and C.-K.Z. participated in the IHC experiment. S.K. and J.-Y.K. participated in molecular and genetic experiments. K.J.R. performed HPLC analysis. Y.-Q.L. and H.L. supervised EM and IHC analysis. Z.-F.C. supervised the project. X.-Y.L. and Z.-F.C. wrote the paper, and W.K.A.K., J.J., Z.-Q.Z., K.J.R., Y.-Q.L., and N.G. contributed to the writing of the paper.

ACKNOWLEDGMENTS

We are grateful to Y.Z.T., A.A.K., R.K., J.Y., X.L.M., Q.T.M., N.H., and Q.F.L. for technical help and members of the Chen laboratory for comments. The project was supported by a NIAMS grant AR056318-01 (Z.-F.C.), a NIH grant R01 DA019921 (K.J.R.), the National Natural Science Foundation of China grants 81371239 and 31371211 (H.L. and Y.-Q.L.), and NIH grants GM069027 and GM080558 (N.G.).

Accepted: September 26, 2014

Published: October 30, 2014

REFERENCES

Abe, K., Kato, G., Katafuchi, T., Tamae, A., Furue, H., and Yoshimura, M. (2009). Responses to 5-HT in morphologically identified neurons in the rat substantia gelatinosa in vitro. *Neuroscience* 159, 316–324.

Akiyama, T., Iodi Carstens, M., and Carstens, E. (2011). Transmitters and pathways mediating inhibition of spinal itch-signaling neurons by scratching and other counterstimuli. *PLoS ONE* 6, e22665.

Akiyama, T., Tominaga, M., Takamori, K., Carstens, M.I., and Carstens, E. (2014). Roles of glutamate, substance P, and gastrin-releasing peptide as spinal neurotransmitters of histaminergic and nonhistaminergic itch. *Pain* 155, 80–92.

Bardin, L. (2011). The complex role of serotonin and 5-HT receptors in chronic pain. *Behav. Pharmacol.* 22, 390–404.

Barnes, N.M., and Sharp, T. (1999). A review of central 5-HT receptors and their function. *Neuropharmacology* 38, 1083–1152.

Basbaum, A.I., and Fields, H.L. (1984). Endogenous pain control systems: brainstem spinal pathways and endorphin circuitry. *Annu. Rev. Neurosci.* 7, 309–338.

Birdsall, T.C. (1998). 5-Hydroxytryptophan: a clinically-effective serotonin precursor. *Altern. Med. Rev.* 3, 271–280.

Björklund, A., Baumgarten, H.G., and Rensch, A. (1975). 5,7-Dihydroxytryptamine: improvement of its selectivity for serotonin neurons in the CNS by pretreatment with desipramine. *J. Neurochem.* 24, 833–835.

Bouvier, M. (2001). Oligomerization of G-protein-coupled transmitter receptors. *Nat. Rev. Neurosci.* 2, 274–286.

Davidson, S., Zhang, X., Khasabov, S.G., Simone, D.A., and Giesler, G.J., Jr. (2009). Relief of itch by scratching: state-dependent inhibition of primate spinothalamic tract neurons. *Nat. Neurosci.* 12, 544–546.

Dillon, S.R., Sprecher, C., Hammond, A., Bilsborough, J., Rosenfeld-Franklin, M., Presnell, S.R., Haugen, H.S., Maurer, M., Harder, B., Johnston, J., et al. (2004). Interleukin 31, a cytokine produced by activated T cells, induces dermatitis in mice. *Nat. Immunol.* 5, 752–760.

Ding, Y.Q., Marklund, U., Yuan, W., Yin, J., Wegman, L., Ericson, J., Deneris, E., Johnson, R.L., and Chen, Z.F. (2003). Lmx1b is essential for the development of serotonergic neurons. *Nat. Neurosci.* 6, 933–938.

Grudt, T.J., Williams, J.T., and Travaglini, R.A. (1995). Inhibition by 5-hydroxytryptamine and noradrenaline in substantia gelatinosa of guinea-pig spinal trigeminal nucleus. *J. Physiol.* 485, 113–120.

Hampton, L.L., Ladenheim, E.E., Akeson, M., Way, J.M., Weber, H.C., Sutliff, V.E., Jensen, R.T., Wine, L.J., Arnheiter, H., and Battey, J.F. (1998). Loss of bombesin-induced feeding suppression in gastrin-releasing peptide receptor-deficient mice. *Proc. Natl. Acad. Sci. USA* 95, 3188–3192.

Heisler, L.K., Chu, H.M., Brennan, T.J., Danao, J.A., Bajwa, P., Parsons, L.H., and Tecott, L.H. (1998). Elevated anxiety and antidepressant-like responses in serotonin 5-HT1A receptor mutant mice. *Proc. Natl. Acad. Sci. USA* 95, 15049–15054.

Hoyer, D., Hannon, J.P., and Martin, G.R. (2002). Molecular, pharmacological and functional diversity of 5-HT receptors. *Pharmacol. Biochem. Behav.* 71, 533–554.

Ikoma, A., Steinhoff, M., Ständer, S., Yosipovitch, G., and Schmelz, M. (2006). The neurobiology of itch. *Nat. Rev. Neurosci.* 7, 535–547.

Jeffry, J.A., Yu, S.Q., Sikand, P., Parihar, A., Evans, M.S., and Premkumar, L.S. (2009). Selective targeting of TRPV1 expressing sensory nerve terminals in the spinal cord for long lasting analgesia. *PLoS ONE* 4, e7021.

Jeffry, J., Kim, S., and Chen, Z.F. (2011). Itch signaling in the nervous system. *Physiology (Bethesda)* 26, 286–292.

Jensen, R.T., Battey, J.F., Spindel, E.R., and Benya, R.V. (2008). International Union of Pharmacology. LXVIII. Mammalian bombesin receptors: nomenclature, distribution, pharmacology, signaling, and functions in normal and disease states. *Pharmacol. Rev.* 60, 1–42.

Julius, D., and Nathans, J. (2012). Signaling by sensory receptors. *Cold Spring Harb. Perspect. Biol.* 4, a005991.

Karunaratne, W.K., Giri, L., Kalyanaraman, V., and Gautam, N. (2013). Optically triggering spatiotemporally confined GPCR activity in a cell and programming neurite initiation and extension. *Proc. Natl. Acad. Sci. USA* 110, E1565–E1574.

Kim, J.Y., Kim, A., Zhao, Z.Q., Liu, X.Y., and Chen, Z.F. (2014). Postnatal maintenance of the 5-HT1a-Pet1 autoregulatory loop by serotonin in the raphe nuclei of the brainstem. *Mol. Brain* 7, 48.

Kroog, G.S., Jensen, R.T., and Battey, J.F. (1995). Mammalian bombesin receptors. *Med. Res. Rev.* 15, 389–417.

Lagerström, M.C., Rogoz, K., Abrahamson, B., Persson, E., Reinius, B., Nordenankar, K., Olund, C., Smith, C., Mendez, J.A., Chen, Z.F., et al. (2010). VGLUT2-dependent sensory neurons in the TRPV1 population regulate pain and itch. *Neuron* 68, 529–542.

LaMotte, R.H., Dong, X., and Ringkamp, M. (2014). Sensory neurons and circuits mediating itch. *Nat. Rev. Neurosci.* 15, 19–31.

Li, J.L., Kaneko, T., Shigemoto, R., and Mizuno, N. (1997). Distribution of trigeminothalamic and spinothalamic tract neurons displaying substance P receptor-like immunoreactivity in the rat. *J. Comp. Neurol.* 378, 508–521.

Liu, Q., Tang, Z., Surdenikova, L., Kim, S., Patel, K.N., Kim, A., Ru, F., Guan, Y., Weng, H.J., Geng, Y., et al. (2009). Sensory neuron-specific GPCR Mrgprs are itch receptors mediating chloroquine-induced pruritus. *Cell* 139, 1353–1365.

Liu, X.Y., Liu, Z.C., Sun, Y.G., Ross, M., Kim, S., Tsai, F.F., Li, Q.F., Jeffry, J., Kim, J.Y., Loh, H.H., and Chen, Z.F. (2011). Unidirectional cross-activation of GRPR by MOR1D uncouples itch and analgesia induced by opioids. *Cell* 147, 447–458.

Liu, X.Y., Wan, L., Huo, F.Q., Barry, D.M., Li, H., Zhao, Z.Q., and Chen, Z.F. (2014). B-type natriuretic peptide is neither itch-specific nor functions upstream of the GRP-GRPR signaling pathway. *Mol. Pain* 10, 4.

Lu, Y., and Perl, E.R. (2007). Selective action of noradrenaline and serotonin on neurones of the spinal superficial dorsal horn in the rat. *J. Physiol.* 582, 127–136.

Ma, Q. (2010). Labeled lines meet and talk: population coding of somatic sensations. *J. Clin. Invest.* 120, 3773–3778.

Millan, M.J. (2002). Descending control of pain. *Prog. Neurobiol.* 66, 355–474.

Milligan, G. (2013). The prevalence, maintenance, and relevance of G protein-coupled receptor oligomerization. *Mol. Pharmacol.* 84, 158–169.

Miyamoto, T., Nojima, H., Shinkado, T., Nakahashi, T., and Kuraishi, Y. (2002). Itch-associated response induced by experimental dry skin in mice. *Jpn. J. Pharmacol.* 88, 285–292.

Mochizuki, H., Tashiro, M., Kano, M., Sakurada, Y., Itoh, M., and Yanai, K. (2003). Imaging of central itch modulation in the human brain using positron emission tomography. *Pain* 105, 339–346.

- Moore, G.A., McConkey, D.J., Kass, G.E., O'Brien, P.J., and Orrenius, S. (1987). 2,5-Di(tert-butyl)-1,4-benzohydroquinone—a novel inhibitor of liver microsomal Ca²⁺ sequestration. *FEBS Lett.* **224**, 331–336.
- Murray, F.S., and Weaver, M.M. (1975). Effects of ipsilateral and contralateral counterirritation on experimentally produced itch in human beings. *J. Comp. Physiol. Psychol.* **89**, 819–826.
- Nattkemper, L.A., Zhao, Z.Q., Nichols, A.J., Papoiu, A.D., Shively, C.A., Chen, Z.F., and Yosipovitch, G. (2013). Overexpression of the gastrin-releasing peptide in cutaneous nerve fibers and its receptor in the spinal cord in primates with chronic itch. *J. Invest. Dermatol.* **133**, 2489–2492.
- O'Donohue, T.L., Massari, V.J., Pazoles, C.J., Chronwall, B.M., Shults, C.W., Quirion, R., Chase, T.N., and Moody, T.W. (1984). A role for bombesin in sensory processing in the spinal cord. *J. Neurosci.* **4**, 2956–2962.
- Ossipov, M.H., Dussor, G.O., and Porreca, F. (2010). Central modulation of pain. *J. Clin. Invest.* **120**, 3779–3787.
- Pang, Y.W., Li, J.L., Nakamura, K., Wu, S., Kaneko, T., and Mizuno, N. (2006). Expression of vesicular glutamate transporter 1 immunoreactivity in peripheral and central endings of trigeminal mesencephalic nucleus neurons in the rat. *J. Comp. Neurol.* **498**, 129–141.
- Paus, R., Schmelz, M., Bíró, T., and Steinhoff, M. (2006). Frontiers in pruritus research: scratching the brain for more effective itch therapy. *J. Clin. Invest.* **116**, 1174–1186.
- Pin, J.P., Neubig, R., Bouvier, M., Devi, L., Filizola, M., Javitch, J.A., Lohse, M.J., Milligan, G., Palczewski, K., Parmentier, M., and Spedding, M. (2007). International Union of Basic and Clinical Pharmacology. LXVII. Recommendations for the recognition and nomenclature of G protein-coupled receptor heteromultimers. *Pharmacol. Rev.* **59**, 5–13.
- Prezeau, L., Rives, M.L., Comps-Agrar, L., Maurel, D., Kniazeff, J., and Pin, J.P. (2010). Functional crosstalk between GPCRs: with or without oligomerization. *Curr. Opin. Pharmacol.* **10**, 6–13.
- Prinster, S.C., Hague, C., and Hall, R.A. (2005). Heterodimerization of g protein-coupled receptors: specificity and functional significance. *Pharmacol. Rev.* **57**, 289–298.
- Sorkin, L.S., and McAdoo, D.J. (1993). Amino acids and serotonin are released into the lumbar spinal cord of the anesthetized cat following intradermal capsaicin injections. *Brain Res.* **607**, 89–98.
- Sun, Y.G., and Chen, Z.F. (2007). A gastrin-releasing peptide receptor mediates the itch sensation in the spinal cord. *Nature* **448**, 700–703.
- Sun, Y.G., Zhao, Z.Q., Meng, X.L., Yin, J., Liu, X.Y., and Chen, Z.F. (2009). Cellular basis of itch sensation. *Science* **325**, 1531–1534.
- Suzuki, R., Rygh, L.J., and Dickenson, A.H. (2004). Bad news from the brain: descending 5-HT pathways that control spinal pain processing. *Trends Pharmacol. Sci.* **25**, 613–617.
- Takanami, K., Sakamoto, H., Matsuda, K.I., Satoh, K., Tanida, T., Yamada, S., Inoue, K., Oti, T., Sakamoto, T., and Kawata, M. (2014). Distribution of gastrin-releasing peptide in the rat trigeminal and spinal somatosensory systems. *J. Comp. Neurol.* **522**, 1858–1873.
- Tominaga, M., Ogawa, H., and Takamori, K. (2009). Histological characterization of cutaneous nerve fibers containing gastrin-releasing peptide in NC/Nga mice: an atopic dermatitis model. *J. Invest. Dermatol.* **129**, 2901–2905.
- Uchizono, K. (1965). Characteristics of excitatory and inhibitory synapses in the central nervous system of the cat. *Nature* **207**, 642–643.
- Walther, D.J., Peter, J.U., Bashammakh, S., Hörtnagl, H., Voits, M., Fink, H., and Bader, M. (2003). Synthesis of serotonin by a second tryptophan hydroxylase isoform. *Science* **299**, 76.
- Ward, L., Wright, E., and McMahon, S.B. (1996). A comparison of the effects of noxious and innocuous counterstimuli on experimentally induced itch and pain. *Pain* **64**, 129–138.
- Yaksh, T.L., and Tyce, G.M. (1981). Release of norepinephrine and serotonin in cat spinal cord: direct in vivo evidence for the activation of descending monoamine pathways by somatic stimulation. *J. Physiol. (Paris)* **77**, 483–487.
- Yoshimura, M., and Furue, H. (2006). Mechanisms for the anti-nociceptive actions of the descending noradrenergic and serotonergic systems in the spinal cord. *J. Pharmacol. Sci.* **101**, 107–117.
- Yosipovitch, G., and Papoiu, A.D.P. (2008). What causes itch in atopic dermatitis? *Curr. Allergy Asthma Rep.* **8**, 306–311.
- Yosipovitch, G., Duque, M.I., Fast, K., Dawn, A.G., and Coghill, R.C. (2007). Scratching and noxious heat stimuli inhibit itch in humans: a psychophysical study. *Br. J. Dermatol.* **156**, 629–634.
- Zhang, Y.Q., Gao, X., Ji, G.C., Huang, Y.L., Wu, G.C., and Zhao, Z.Q. (2002). Expression of 5-HT1A receptor mRNA in rat lumbar spinal dorsal horn neurons after peripheral inflammation. *Pain* **98**, 287–295.
- Zhao, Z.Q., Scott, M., Chiechio, S., Wang, J.S., Renner, K.J., Gereau, R.W., 4th, Johnson, R.L., Deneris, E.S., and Chen, Z.F. (2006). Lmx1b is required for maintenance of central serotonergic neurons and mice lacking central serotonergic system exhibit normal locomotor activity. *J. Neurosci.* **26**, 12781–12788.
- Zhao, Z.Q., Chiechio, S., Sun, Y.G., Zhang, K.H., Zhao, C.S., Scott, M., Johnson, R.L., Deneris, E.S., Renner, K.J., Gereau, R.W., 4th, and Chen, Z.F. (2007a). Mice lacking central serotonergic neurons show enhanced inflammatory pain and an impaired analgesic response to antidepressant drugs. *J. Neurosci.* **27**, 6045–6053.
- Zhao, Z.Q., Gao, Y.J., Sun, Y.G., Zhao, C.S., Gereau, R.W., 4th, and Chen, Z.F. (2007b). Central serotonergic neurons are differentially required for opioid analgesia but not for morphine tolerance or morphine reward. *Proc. Natl. Acad. Sci. USA* **104**, 14519–14524.
- Zhao, Z.-Q., Huo, F.-Q., Jeffrey, J., Hampton, L., Demehri, S., Kim, S., Liu, X.-Y., Barry, D.M., Wan, L., Liu, Z.-C., et al. (2013). Chronic itch development in sensory neurons requires BRAF signaling pathways. *J. Clin. Invest.* **123**, 4769–4780.
- Zhao, Z.Q., Wan, L., Liu, X.Y., Huo, F.Q., Li, H., Barry, D.M., Krieger, S., Kim, S., Liu, Z.C., Xu, J., et al. (2014). Cross-Inhibition of NMBR and GRPR Signaling Maintains Normal Histaminergic Itch Transmission. *J. Neurosci.* **34**, 12402–12414.

Neuron, Volume 84

Supplemental Information

Descending Control of Itch Transmission by the Serotonergic System via 5-HT_{1A}-Facilitated GRP-

GRPR Signaling

Zhong-Qiu Zhao, Xian-Yu Liu, Joseph Jeffry, W.K. Ajith Karunaratne, Jin-Lian Li, Admire Munanairi, Xuan-Yi Zhou, Hui Li, Yan-Gang Sun, Li Wan, Zhen-Yu Wu, Seungil Kim, Fu-Quan Huo, Ping Mo, Devin M Barry, Chun-Kui Zhang, Ji-Young Kim, N. Gautam, Kenneth J. Renner, Yun-Qing Li, and Zhou-Feng Chen

Figure S1, Related to Figure 1

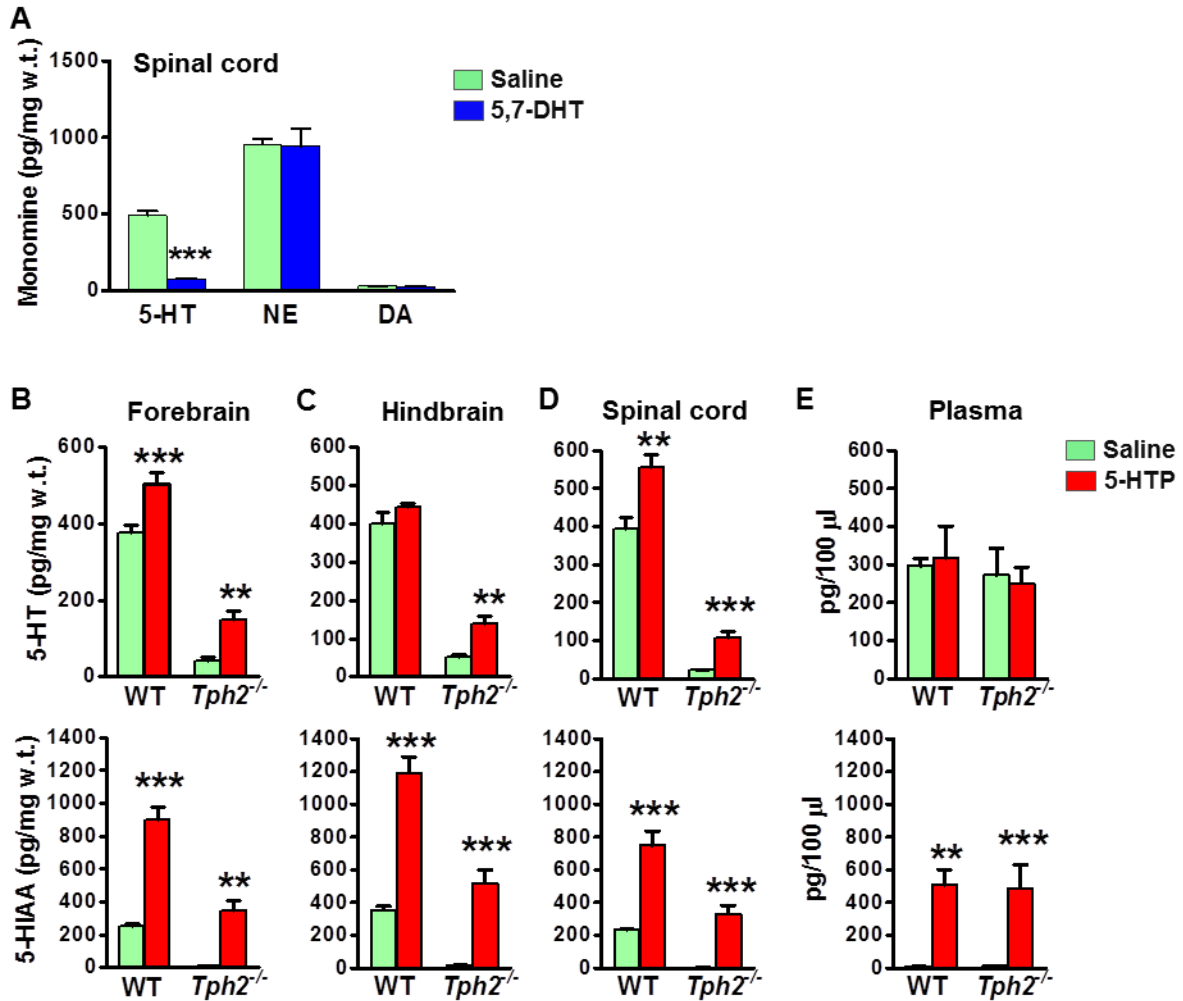


Figure S2, Related to Figure 3

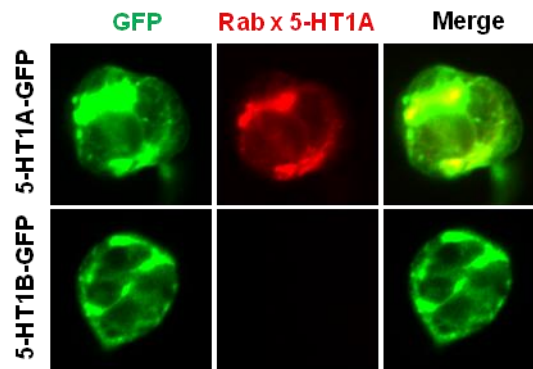


Figure S3, Related to Figure 3

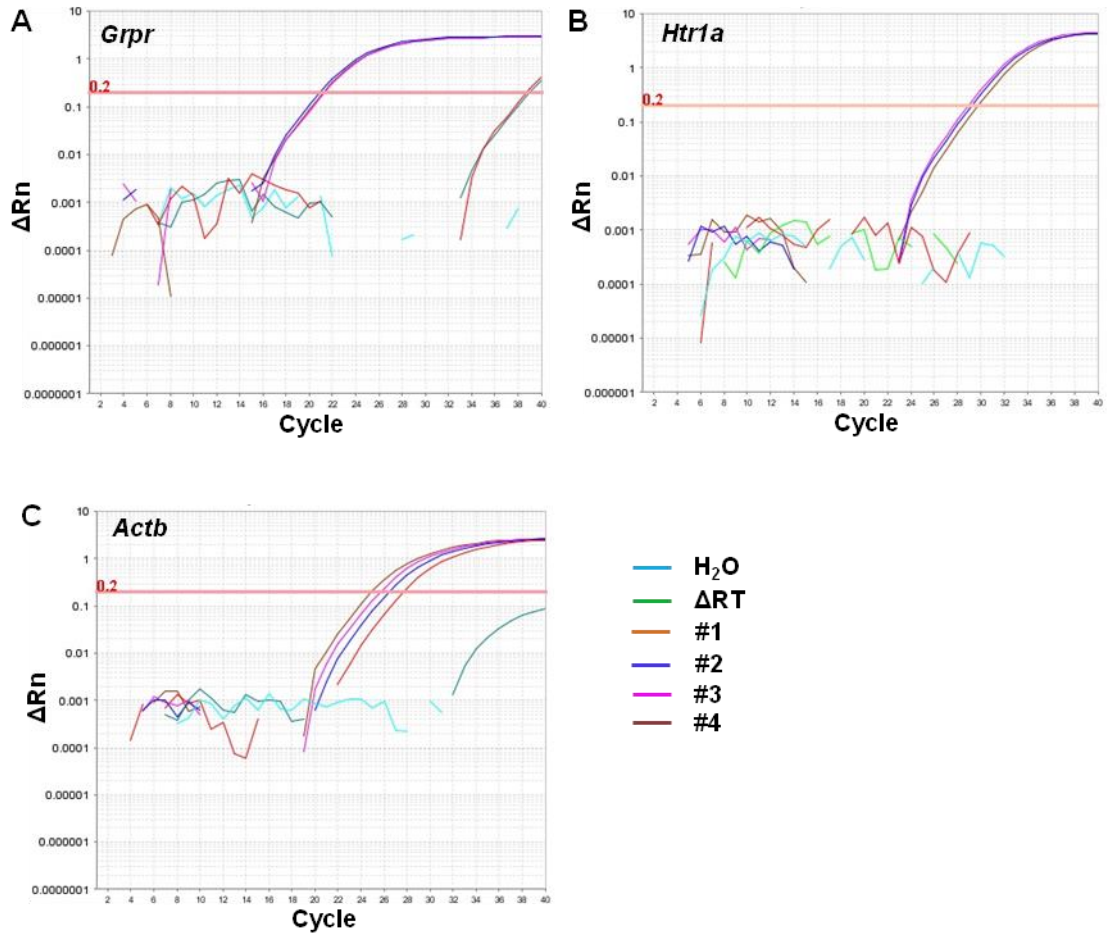


Figure S4, Related to Figure 4

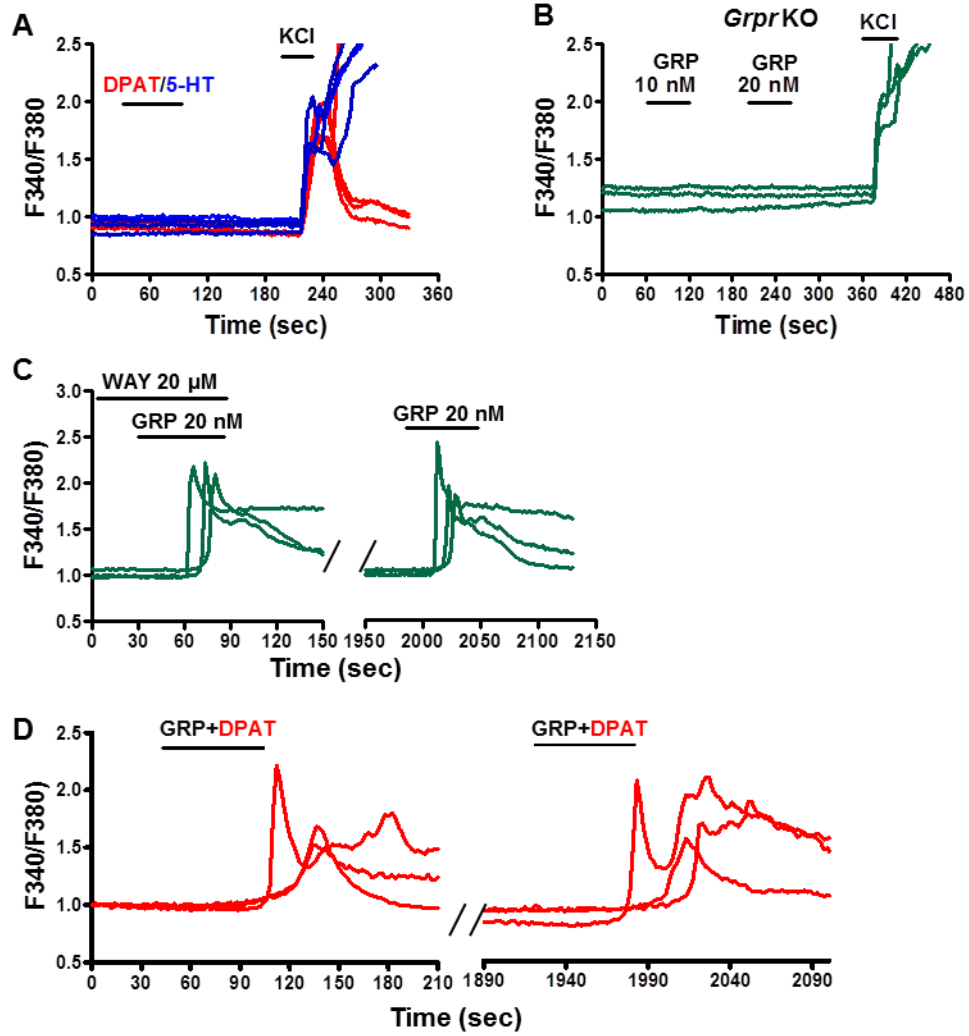


Figure S5, Related to Figure 5

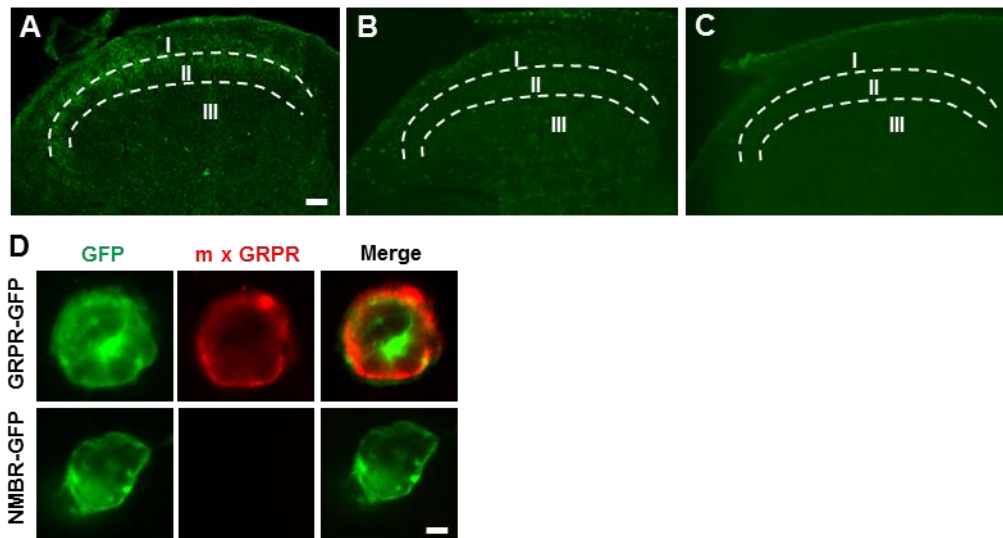


Figure S7, Related to Figure 7

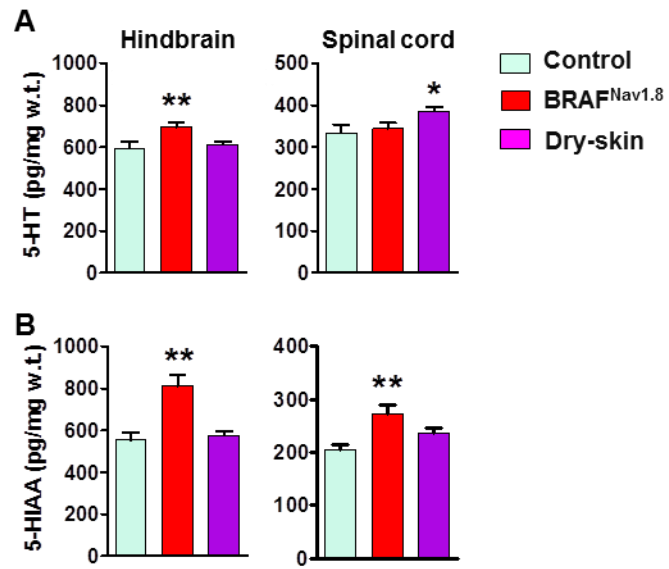


Table S1, Related to Figure 3

Cell #	Δ RT	#1	#2	#3	#4	#5	#6	#7	#8	#9	#10
<i>Actb</i>	-	+	+	+	+	+	+	+	+	+	+
<i>Grpr</i>	-	-	+	+	+	+	+	+	+	+	+
<i>Htr1a</i>	-	-	+	+	+	-	+	+	+	-	+

SUPPLEMENTAL FIGURE LEGENDS

Figure S1. Reduced Spinal 5-HT Level after 5,7-DHT Injection and Enhanced Central 5-HT Concentrations by Systemic 5-HTP Administration, Related to Figure 1.

(A) Spinal 5-HT level was significantly reduced after 5,7-DHT treatment as detected by HPLC, while the levels of noradrenaline (NE) and dopamine (DA) were not affected.

(B-E) The concentrations of 5-HT (upper row) and 5-HIAA (lower row) in the forebrain (B), hindbrain (C), spinal cord (D) and plasma (E) were detected by HPLC with electrochemical detection. n = 4-5.

Error bars represent SEM. **p < 0.01, ***p < 0.001, versus saline.

Figure S2. 5-HT1A Antibody Is Specific, Related to Figure 3.

Rabbit anti-5-HT1A antibody (Rab x 5-HT1A) specifically labeled HEK 293 cell expressing 5-HT1A-GFP (red, upper row), but not 5-HT1B-GFP (lower row). Successful expression of 5-HT1A-GFP and 5-HT1B-GFP was confirmed by GFP fluorescence (green).

Figure S3. Co-Expression of *Grpr* and *Htr1a* in GRPR-eGFP Neurons, Related to Figure 3.

(A and B) qRT-PCR traces showing that *Grpr* (A) and *Htr1a* (B) were detected in 3 spinal GRPR-eGFP neurons (#2 - #4), but not in 1 spinal NMBR-eGFP neuron (#1).

(C) *Actb* mRNA was detectable in all 4 neurons.

Specificity of the PCR reactions were verified using two negative controls, in which cDNA was substituted with H₂O or no RT product (Δ RT).

Figure S4. GRP, 8-OH-DPAT and WAY100635 Are Specific, Related to Figure 4.

(A) 5-HT (blue traces) or 8-OH-DPAT (DPAT, red traces) was not able to induce Ca²⁺ response in dissociated WT spinal neurons.

(B) Up to 20 nM of GRP didn't evoke Ca²⁺ response in dissociated spinal neurons of *Grpr* KO mice.

(C) WAY100635 failed to block GRP-evoked Ca^{2+} spikes in dissociated WT spinal neurons.

(D) WT spinal neurons showed comparable Ca^{2+} response to two times of co-application of GRP (5 nM) and 8-OH-DPAT (10 μM) with 30 min wash in between.

Figure S5. The specificity Test of Mouse Anti-GRPR Monoclonal Antibody, Related to Figure 5.

(A) GRPR antibody staining on WT mouse spinal dorsal horn.

(B) GRPR antibody staining on bombesin-saporin treated mouse.

(C) GRPR staining after GRPR antigen adsorption.

(D) Mouse anti-GRPR antibody (mxGRPR) specifically labeled HEK 293 cells expressing GRPR-GFP (upper row) but not NMBR-GFP (lower row).

Scale bars, 100 μm in A, 20 μm in D.

Figure S6. No Detectable FRET Was Observed Between GRPR-eGFP and 5-HT1B-mCh, Related to Figure 5.

(A) Representative confocal images showing plasma membrane fluorescence intensities of HEK293 cells expressing 5HT-1B-mCherry (red) and GRPR-eGFP (green), before and after acceptor (mCh) photobleaching in the selected region of a cell (yellow box), Overlay images show typical example of a cell co-expressing 5HT-1B-mCh and GRPR-eGFP. Scale bar, 10 μm .

(B) Top: Plots showing background subtracted normalized fluorescence intensities of donor excitation/donor emission (green trace, 488 nm excitation, 515 nm emission: DD), donor excitation/acceptor emission (red trace, 488 nm excitation, 630 nm emission: DA) and acceptor excitation/acceptor emission (pink trace, 595 nm excitation, 630 nm emission: AA) from selected plasma membrane regions of the cells that were photobleached. Bottom: Averaged FRET ratio (DA/DD) in the photobleached regions. $n = 9-11$. Error bars represent SEM.

(C) Background subtracted normalized fluorescence intensities (top) and averaged FRET ratio (bottom) of non-photobleached regions in (A).

Figure S7. Enhanced 5-HT Level in Mice with Chronic Itch, Related to Figure 7.

(A) The level of 5-HT was significantly upregulated in hindbrain of BRAF^{Nav1.8} mice and in the spinal cord of dry-skin mice.

(B) BRAF^{Nav1.8} mice showed enhanced level of 5-HIAA in both hindbrain and the spinal cord.

Table S1. Expression of *Grpr* and *Htr1a* in GRPR-eGFP⁺ Spinal Neurons.

Grpr message was detected in all GRPR-eGFP⁺ superficial dorsal horn neurons (#2-10) by single cell RT-PCR. *Htr1a* signal was detected in 7 out of 9 GRPR-eGFP⁺ neurons (#2-4, 6, 7, 10). No *Grpr* or *Htr1a* expression was detected in Δ RT control or one NMBR-eGFP spinal neuron (#1).

SUPPLEMENTAL EXPERIMENTAL PROCEDURES

Mice

Adult male C57BL/6J mice, *Lmx1b*^{fl/p} mice (Ding et al., 2003), *Tph2*^{-/-} mice (Kim et al., 2014), *Htr1a*^{-/-} mice (Heisler et al., 1998), *Grpr* KO mice (Hampton et al., 1998) and BRAF^{Nav1.8} mice (Zhao et al., 2013) were used for the study.

All mouse strains were maintained in a congenic C57BL/6J background and their wild-type littermates were used as controls for all experiments. C57BL/6J male mice (Jackson Laboratory) were also used for pharmacological studies. Mice were housed in clear plastic cages in a controlled environment at a constant temperature of 23°C and humidity of 50% \pm 10% with food and water available *ad libitum*. The animal room was on a 12/12 h light/dark cycle with lights on at 0700. Male mice 7 to 12 weeks old were used to test for behavior and staining. Experimental procedures were conducted in accordance with policies of the National Institutes of Health and were approved by the Animal Studies Committee at Washington University School of Medicine.

Drugs and Chemicals

CQ, 5,7-DHT, 5-HTP, (R)-(+)-8-OH-DPAT (5-HT_{1A} agonist), DOI (5-HT_{2A} agonist), BW 723C86 (5-HT_{2B} agonist), α -ME-5-HT (5-HT₂ agonist), 1-(3-Chlorophenyl) biguanide hydrochloride (m-CPBG, 5-HT₃ agonist) and WAY100635 were purchased from Sigma-Aldrich (St. Louis, MO). GRP₁₈₋₂₇ was purchased from Bachem (King of Prussia, PA). CP 93129 (5-HT_{1B} agonist), LY344864 (5-HT_{1F} agonist), m-cpp (5-HT_{2C} agonist), RS 67506 (5-HT₄ agonist), EMD 386088 (5-HT₆ agonist) and AS 19 (5-HT₇ agonist) were purchased from R&D Systems.

All chemicals were dissolved in sterile saline. The volume of drug solutions was 5 μ L for i.t. and i.c. injections and 50 μ L for nape i.d. injections. The dose chosen was based on our previous work (Sun and Chen, 2007; Sun et al., 2009) or determined in pilot experiments on a small group of animals. The doses of drugs were as follows: CQ, 200 μ g nape i.d; 5-HTP, 10 mg/kg, i.p.; 5-HT receptor agonists, 5 nmol, i.t.; Other detailed information for time and doses for their use was indicated in results or figure legends.

Acute Scratching Behavior

Scratching behaviors were performed as previously described (Sun and Chen, 2007; Sun et al., 2009). Briefly, the injection area was shaved two days before experiments. To avoid cross-tachyphylaxis, each mouse was used for just one test. Prior to the experiments, each mouse was placed in a plastic arena (10 \times 11 \times 15 cm) for 30 min to acclimate. Mice were briefly removed from the chamber for injection. Animal behaviors were videotaped (SONY HDR-CX190) from a side angle and played back on computer for assessments by observers blinded to the treatments and the genotypes of the animals. Hind limb scratching behavior towards the injected area was observed for 30 min with 5 min intervals. One bout of scratch was defined as a lifting of the hind limb to the injection site and then a replacing of the limb back to the floor or to the mouth, regardless of how many scratching strokes took place in between (Sun and Chen, 2007).

Intradermal (i.d.) Injection: The injections were performed as previously described (Shimada and LaMotte, 2008). Pruritogen of 50 μ L was injected intradermally into the nape of neck.

Intracisternal (i.c.) Injection: The i.c. injection was performed as described earlier (Reijneveld et al., 1999). Briefly, the animal was placed in the prone position with their neck draped over a 15 mL cylinder. A volume of 5 μ L solution was injected using a Hamilton syringe between the occiput and C₁ while mouse head was immobilized by the performer's thumb and midfinger.

Intrathecal (i.t.) Injection: Intrathecal injections into the lumbar region of unanaesthetized mice were performed as described previously (Hylden and Wilcox, 1980). Briefly, 30-gauge needle attached on 10 μ L-Hamilton Syringe was inserted into the intervertebral space between L5 and L6. Drugs were injected in a volume of 10 μ l.

5,7-DHT Treatment

The protocol is similar to literatures (Oatway et al., 2004). Endogenous spinal 5-HT fibers were ablated in C57BL/6J mice using 5,7-dihydroxy-tryptamine (5,7-DHT)(Sigma-Aldrich). To prevent the uptake of 5,7-DHT into noradrenergic neurons, mice were pre-treated with desipramine hydrochloride (Sigma-Aldrich)(25 mg/kg, i.p.) for 45 min. Mice were then administrated with either 5,7-DHT (20 μ g, i.t.) or vehicle (0.9% saline, 5 μ l). Behavioral tests were performed 2 weeks after 5,7-DHT injection. The spinal cords were then dissected out for monoamines measurements using HPLC.

Immunohistochemistry and *in situ* Hybridization

Immunohistochemical staining and *in situ* hybridization were performed as previously described (Zhao et al., 2006). Briefly, mice were anesthetized with an overdose of ketamine, and fixed by intracardiac perfusion with cold PBS (0.01M, pH 7.4) followed by 4% paraformaldehyde. The brain, spinal cord and small intestine were immediately removed, postfixed in the same fixative overnight at 4 °C and cryoprotected in 30% sucrose solution. Frozen tissue was sectioned at 20~25 μ m thickness using a cryostat. Free-floating sections were blocked in a solution containing 2% donkey serum and 0.3% Triton X-100 in PBS for 1 h at room temperature. The sections were incubated with primary antibodies overnight at 4 °C followed by the use of FITC or Cy3-conjugated secondary antibodies (Jackson

ImmunoResearch). The following primary antibodies were used: rabbit anti-5-HT (1:5,000, Immunostar), rabbit anti-5-HT1A (1:200, Santa Cruz) and chicken anti-GFP (polyclonal, 1:500, Aves Labs). For the *in situ* hybridization study, a digoxigenin-labeled cRNA probe was used as described earlier (Zhao et al., 2006). Images were taken using a Nikon Eclipse Ti-U microscope.

Small Interfering RNA Treatment

Negative control siRNA (SIC001) and selective siRNA duplex for mouse *Htr1a* mRNA knock-down (SASI_Mm01_00197594) were purchased from Sigma. RNA was dissolved in diethyl pyrocarbonate-treated PBS and prepared immediately prior to administration by mixing the RNA solution with a transfection reagent, *in vivo*-jet PEI[®] (Polyplus-transfection SA). The final concentration of RNA was 1.25 µg/10 µl. siRNA was delivered to the lumbar region of the spinal cord. Injection was given twice daily for 6 consecutive days as described previously with some modifications (Kawasaki et al., 2008; Liu et al., 2011; Luo et al., 2005; Tan et al., 2005). Behavior testing was carried out at 24 h after the last injection.

Immune-Electron Microscopy

Immune-electron microscopic studies were performed as previously described (Li et al., 1997; Pang et al., 2006). Briefly, three adult male GRPR-eGFP mice were perfused transcardially with 4% paraformaldehyde. Lumbar enlargement of spinal cord was cut serially into 50-µm thick cross sections on a vibratome (Microslicer DTM-1000; Dosaka EM, Kyoto, Japan). Subsequently, 5-HT and GFP were labeled by the immunogold–silver method and by the immunoperoxidase method, respectively. The sections were incubated with a mixture of rabbit anti-5-HT antibody (1:2,000; Incstar Corporation, Stillwater, MN) and guinea pig anti-GFP antibody (1.5 µg/ml) (Nakamura et al., 2008) at room temperature for 24 h followed by a mixture of 1.4-nm gold-particle-conjugated goat anti-rabbit IgG (1:100, Nanoprobes, 2003, Stony Brook, NY) and biotinylated donkey anti-guinea pig IgG (1:100, 706-065-148; Jackson Immunoresearch, West Grove, PA). The sections were then postfixed with 1% (w/v)

glutaraldehyde in 0.1 M PB (pH 7.4) for 10 min and washed in distilled water. Subsequently, silver enhancement was done in the dark with HQ Silver Kit (2012; Nanoprobes). Then the sections were incubated with avidin-biotin-peroxidase complex (1:50, Elite ABC Kit; Vector) for 6 hrs. Next, the sections were incubated in 0.05 M Tris-HCl (pH 7.6) containing 0.02% (w/v) DAB (Dojindo, Tokyo, Japan) and 0.003% (v/v) H₂O₂ for 20–30 min at room temperature. Then the sections were osmated, counterstained with 1% (w/v) uranyl acetate, dehydrated, embedded as described previously (Pang et al., 2006). Further, 50-nm-thick ultrathin sections were cut with a diamond knife mounted on an ultramicrotome and examined with a JEM-1400 electron microscope (JEM, Tokyo, Japan). The digital micrographs were captured by VELETA (Olympus, Tokyo, Japan).

HPLC

The concentrations of monoamines (5-HT, NE, DA and 5-HIAA) were measured using HPLC with electrochemical detection as previously described (Zhao et al., 2006). Briefly, mice were anesthetized with an overdose of ketamine, and their brains and spinal cords were immediately removed and frozen on dry ice. The brains were divided into the rostral and caudal halves at the juncture of the medulla/pons region. Blood was taken from the heart and centrifuged at 12,000 rpm for 10 min at 4°C to separate plasma from blood cells. The concentrations of the amines were calculated with respect to the mean peak height values obtained from standard runs set in the internal standard mode using CSW32 software (DataApex, Prague, Czech Republic). The resulting values were corrected for volume and expressed as pg of amine per mg of wet tissue or per 100 µL of plasma. For analyzing the effect of 5-HTP injections on indole amine concentrations, samples were collected one hour after 5-HTP or saline administration.

Single Cell qRT-PCR

Single-cell qRT-PCR was carried out using Ambion® Single Cell-to-CT™ Kit (Life technologies) in accordance with manufactures instructions. Briefly, single eGFP⁺ neuron in lamina I of spinal cord

slices from GRPR-eGFP mouse or NMBR-eGFP mouse was identified by green fluorescence under microscope. Negative pressure was applied to the pipette to isolate cytosol of the cell, which was extruded into 10 μ l cell lysis/Dnase I solution for RNA extraction and genomic DNA digestion. After reverse transcription (25°C, 10 min/42°C, 60 min/85°C, 5 min) target cDNA was pre-amplified for 14 cycles (95°C, 15 sec/60°C, 4min) in the presence of 0.2x pooled TaqMan assays (Life technologies). One GRPR-eGFP neuron was used as Δ RT control for which reverse transcriptase was omitted at cDNA synthesis step. Diluted pre-amplification products (1:20 in 1x TE buffer) was used for final qPCR reaction (4 μ l, 40 cycles of 95°C 5 sec/60°C 30 sec; StepOnePlus, Applied Biosystems) to examine target gene expression. TaqMan assays used are: *Grpr*, Mm01157247_m1; *Htr1a*, Mm00434106_s1; *Actb*, Mm01205647_g1. Data were analyzed using StepOne Software (v2.2.2.) with automatic baseline and threshold was set to 0.2.

Plasmid

Myc-GRPR, HA-5-HT1A, HA-5-HT1B, GRPR-GFP, 5-HT1A-mCherry, 5-HT1B-mCherry, NMBR-GFP, 5-HT1A-GFP and 5-HT1B-GFP were constructed using polymerase chain reaction and subcloned into a pcDNA3.1 (Life Technologies) using In-Fusion HD kit (Clontech Laboratories, Inc.).

Cell Culture and Transfections

HEK293 cells were grown in Dulbecco's modified Eagle's medium supplemented with 10% fetal bovine serum in a humidified atmosphere containing 5% CO₂. Stable HEK293 cell lines were made as described previously (Liu et al., 2011). Briefly, cells were first transfected with plasmid containing the neomycin resistance by electroporation (GenePulser Xcell, Bio-Rad). Stable transfectants were selected in the presence of 500 μ g/ml G418 (Invitrogen). To generate lines co-expressing two distinct epitope-tagged receptors, the cells were subjected to a second round of transfection and selected in the presence of 500 μ g/ml G418 and 100 μ g/ml hygromycin (Roche). Clones expressing Myc-GRPR, HA-5-HT1A, HA-5-HT1A/Myc-GRPR, and HA-5-HT1B/Myc-GRPR were generated. For FRET

experiments and antibody verification, receptors were transiently transfected into HEK293 cells using Lipofectamine 2000™ (Invitrogen) following the manufacturer's instruction. FRET was done at 37°C 24 h after transfection. GRPR and 5-HT1A antibody staining was carried out 24 h after transfection as described (Liu et al., 2011). Dilution of tested antibodies were 1:200 for rabbit anti-5-HT-1A and 1:1,000 for mouse anti-GRPR.

Dissociation of Spinal Neurons

Primary culture of spinal dorsal horn neurons was prepared from 5-7-days-old C57BL/6J mice (Zhao et al., 2013). After decapitation under deep anesthesia with diethylether, a laminectomy was performed and dorsal horn of spinal cord was dissected out with a razor blade and incubated in Neurobasal-A Medium (Gibco) containing 30 µl papain (Worthington) at 37 °C for 20 min. Enzymatic digestion was stopped by adding another 2 ml Neurobasal-A medium. After washing with the same medium for three times gentle trituration was performed using flame polished glass pipette until solution became cloudy. The homogenate was centrifuged at 1,500 rpm for 5 min and supernatant was discarded. Cell pellets were resuspended in culture medium composed of Neurobasal medium (Gibco, 92% vol/vol), fetal bovine serum (Invitrogen, 2% vol/vol), HI Horse Serum (Invitrogen, 2% vol/vol), GlutaMax (2 mM, Invitrogen, 1% vol/vol), B27 (Invitrogen, 2% vol/vol), Penicillin (100 µg/ml) and Streptomycin (100 µg/ml) and then plated onto 12-mm coverslips coated with poly-D-lysine. After three days neurons were used for calcium imaging studies.

Calcium Imaging

Calcium imaging experiments were performed as described previously (Liu et al., 2011). The cells were loaded with Fura 2-acetomethoxy ester (Molecular Probes) for 30 min at 37°C. After washing, cells were imaged at 340 and 380 nm excitation to detect intracellular free calcium. Calibration was performed using Fura-2 Calcium Imaging Calibration Kit (Invitrogen) following the manufacturer's

instructions. Each experiment was done at least three times and a minimum of 200 cells were analyzed each time.

Co-Immunoprecipitation and Western Blot Analysis

Tissues or cells were lysed in lysis buffer (50 mM Tris-HCl, pH 7.4, 150 mM NaCl, 5 mM EDTA, 1% Nonidet P-40, 0.5% sodium deoxycholate, 0.1% SDS, and proteinase inhibitors) and membrane proteins were prepared as described earlier (Liu et al., 2011). Solubilized samples (200 µg) were incubated with either rabbit antibody against HA (BD bioscience), mouse antibody against c-Myc (Covance) or GRPR (Abmart) overnight at 4 °C. The complex was precipitated with 50% TrueBlot™ anti-rabbit or anti-mouse IgG bead slurry (eBioscience). After washing, the beads were boiled in LDS sample buffer (Invitrogen) with 50 mM dithiothreitol for 10 min. Western blot was carried out with mouse anti Myc (1:1,000), rabbit anti HA (1:1,000), mouse anti-GRPR (1:5,000) or rabbit anti-5-HT1A (1:5,000, Abcam). The GRPR mouse monoclonal antibody was custom-made via Abmart. Specificity of the antibody was validated using different approaches. First, GRPR staining signals were markedly ablated in the superficial dorsal horn of bombesin-saporin-treated mice (Sun et al., 2009; Zhao et al., 2014) (Figure S5B). Second, antigen adsorption completely blocked staining in control spinal sections (Figure S5C). Finally, HEK 293 cells expressing GRPR but not NMBR were specifically labeled by GRPR antibodies (Figure S5D).

Confocal Subcellular FRET Imaging

HEK 293 cells transiently expressing fluorescently tagged receptors were seeded in 29 mm glass bottom dishes. The FRET imaging and calculations were performed as described previously (Karunaratne et al., 2013). Basal FRET between eGFP (donor) and mCherry (acceptor) was measured by rapid photobleaching of the acceptor in a defined region of a single cell (ROI) which expresses both the donor and the acceptor (Figure 5E, yellow box). ROIs were photobleached using Andor FRAP-PA unit. The unbleached region of the same cell was used as control. Laser intensities of

the photobleaching lasers were adjusted using an acoustic tunable optical filter (AOTF) to prevent photobleaching of the donor. Before and after photobleaching, a series of time lapse images were captured with donor excitation-donor emission (DD) and donor excitation-acceptor emission (DA).

Electrophysiological Recording

Spinal cord slices were obtained from GRPR-eGFP mice 3-4 weeks of age. Laminectomies were performed in cold sucrose based solution (in mM): sucrose 300, KCl 2, NaH₂PO₄ 1.25, CaCl₂ 1, MgCl₂ 5, NaHCO₃ 26 and glucose 11. Transverse sections (400 µm) were taken with a vibratome 3000 tissue slicer and transferred to a recovery chamber containing standard artificial cerebrospinal fluid (in mM): NaCl 140, KCl 2.5, NaH₂PO₄ 1.4, CaCl₂ 2, MgCl₂ 2, NaHCO₃ 25 and glucose 11. For recording, slices were transferred to a recording chamber (Warner RC-21G) and continuously perfused (2 ml/min) with ACSF. Drugs were applied via the perfusion system. For Giga-seal whole cell recording, thick wall borosilicate pipettes were pulled (Sutter P-97) to a diameter of 3-5 MΩ and filled with an intracellular solution consisting of (in mM); K gluconate (130), NaCl (10), MgCl₂ (1), EGTA (0.2), HEPES (10), MgATP (1), NaGTP (5). GRPR-eGFP neurons were visualized with an Olympus BX-51 upright microscope and FITC fluorescent filter. Current clamp signals were control and acquired with a multiclamp 700B amplifier, digidata 1440 and pClamp 10 software. Signals were low pass filtered at 2 kHz and digitized at 5 kHz. Firing patterns were examined by injection of steps of positive current for 500 ms. Input resistance was tested every 20 s for drug induced changes by injection of negative (20 pA) current. Membrane depolarizations were measured by subtracting steady state value (mV) under control conditions from the peak value (mV) observed during agonist application conditions. For neurons that fired action potentials in response to agonist application the peak membrane potential value was defined as the AP threshold of the first AP where the slope became greater than 5mV/ms. Series resistance was monitored in voltage clamp mode by measuring the instantaneous current in response to small voltage steps; recordings having greater than 20% change in series resistance were discarded. Data were analyzed offline (clampfit 10) and plotted in Origin 8 graphing software.

Chronic Itch Models

Dry Skin (Xerosis): The dry skin model was set up as described (Akiyama et al., 2010; Miyamoto et al., 2002). Briefly, the nape of mice at 8-12 weeks age was shaved and a mixture of acetone and diethylether (1:1) was painted on the neck skin for 15 sec, followed by 30 sec of distilled water application (AEW). This regiment was administrated twice daily for 10 days. Littermate control mice received water only for 45 sec on the same schedule. Spontaneous scratches were examined on the morning following the last AEW treatment. Baseline scratching behaviors were recorded for 60 min. Mice were returned to home cages for 20 min followed by drug injection. Ten minutes later scratching behaviors were recorded for another 60 min.

Statistical Analysis

All values are expressed as the means \pm standard error of the mean (SEM). Statistical analyses were performed using Prism 5 (version 5.03, GraphPad, San Diego, CA). One-Way Analysis of Variance was used to test the equality of three or more means at one time. For comparison of the mean of two groups a Student's *t* test was used. $p < 0.05$ was considered statistically significant.

SUPPLEMENTAL REFERENCES

Akiyama, T., Carstens, M.I., and Carstens, E. (2010). Enhanced scratching evoked by PAR-2 agonist and 5-HT but not histamine in a mouse model of chronic dry skin itch. *Pain* 151, 378-383.

Ding, Y.Q., Marklund, U., Yuan, W., Yin, J., Wegman, L., Ericson, J., Deneris, E., Johnson, R.L., and Chen, Z.F. (2003). Lmx1b is essential for the development of serotonergic neurons. *Nature neuroscience* 6, 933-938.

- Hampton, L.L., Ladenheim, E.E., Akeson, M., Way, J.M., Weber, H.C., Sutliff, V.E., Jensen, R.T., Wine, L.J., Arnheiter, H., and Battey, J.F. (1998). Loss of bombesin-induced feeding suppression in gastrin-releasing peptide receptor-deficient mice. *Proc Natl Acad Sci U S A* *95*, 3188-3192.
- Heisler, L.K., Chu, H.M., Brennan, T.J., Danao, J.A., Bajwa, P., Parsons, L.H., and Tecott, L.H. (1998). Elevated anxiety and antidepressant-like responses in serotonin 5-HT_{1A} receptor mutant mice. *Proc Natl Acad Sci U S A* *95*, 15049-15054.
- Hylden, J.L., and Wilcox, G.L. (1980). Intrathecal morphine in mice: a new technique. *Eur J Pharmacol* *67*, 313-316.
- Karunaratne, W.K., Giri, L., Kalyanaraman, V., and Gautam, N. (2013). Optically triggering spatiotemporally confined GPCR activity in a cell and programming neurite initiation and extension. *Proc Natl Acad Sci U S A* *110*, E1565-1574.
- Kawasaki, Y., Xu, Z.-Z., Wang, X., Park, J.Y., Zhuang, Z.-Y., Tan, P.-H., Gao, Y.-J., Roy, K., Corfas, G., Lo, E.H., *et al.* (2008). Distinct roles of matrix metalloproteases in the early- and late-phase development of neuropathic pain. *Nat Med* *14*, 331-336.
- Kim, J.Y., Kim, A., Zhao, Z.Q., Liu, X.Y., and Chen, Z.F. (2014). Postnatal maintenance of the 5-HT_{1A}-Pet1 autoregulatory loop by serotonin in the raphe nuclei of the brainstem. *Molecular brain* *7*, 48.
- Li, J.L., Kaneko, T., Shigemoto, R., and Mizuno, N. (1997). Distribution of trigeminohypothalamic and spinohypothalamic tract neurons displaying substance P receptor-like immunoreactivity in the rat. *The Journal of comparative neurology* *378*, 508-521.
- Liu, X.Y., Liu, Z.C., Sun, Y.G., Ross, M., Kim, S., Tsai, F.F., Li, Q.F., Jeffry, J., Kim, J.Y., Loh, H.H., *et al.* (2011). Unidirectional cross-activation of GRPR by MOR1D uncouples itch and analgesia induced by opioids. *Cell* *147*, 447-458.
- Luo, M.-C., Zhang, D.-Q., Ma, S.-W., Huang, Y.-Y., Shuster, S., Porreca, F., and Lai, J. (2005). An efficient intrathecal delivery of small interfering RNA to the spinal cord and peripheral neurons. *Molecular pain* *1*, 29.

- Miyamoto, T., Nojima, H., Shinkado, T., Nakahashi, T., and Kuraishi, Y. (2002). Itch-associated response induced by experimental dry skin in mice. *Jpn J Pharmacol* 88, 285-292.
- Nakamura, K.C., Kameda, H., Koshimizu, Y., Yanagawa, Y., and Kaneko, T. (2008). Production and histological application of affinity-purified antibodies to heat-denatured green fluorescent protein. *The journal of histochemistry and cytochemistry : official journal of the Histochemistry Society* 56, 647-657.
- Oatway, M.A., Chen, Y., and Weaver, L.C. (2004). The 5-HT₃ receptor facilitates allodynia following spinal cord injury. *Pain* 110, 259-268.
- Pang, Y.W., Li, J.L., Nakamura, K., Wu, S., Kaneko, T., and Mizuno, N. (2006). Expression of vesicular glutamate transporter 1 immunoreactivity in peripheral and central endings of trigeminal mesencephalic nucleus neurons in the rat. *The Journal of comparative neurology* 498, 129-141.
- Reijneveld, J.C., Taphoorn, M.J., and Voest, E.E. (1999). A simple mouse model for leptomeningeal metastases and repeated intrathecal therapy. *J Neurooncol* 42, 137-142.
- Shimada, S.G., and LaMotte, R.H. (2008). Behavioral differentiation between itch and pain in mouse. *Pain* 139, 681-687.
- Sun, Y.G., and Chen, Z.F. (2007). A gastrin-releasing peptide receptor mediates the itch sensation in the spinal cord. *Nature* 448, 700-703.
- Sun, Y.G., Zhao, Z.Q., Meng, X.L., Yin, J., Liu, X.Y., and Chen, Z.F. (2009). Cellular basis of itch sensation. *Science* 325, 1531-1534.
- Tan, P.H., Yang, L.C., Shih, H.C., Lan, K.C., and Cheng, J.T. (2005). Gene knockdown with intrathecal siRNA of NMDA receptor NR2B subunit reduces formalin-induced nociception in the rat. *Gene Ther* 12, 59-66.
- Zhao, Z.-Q., Wan, L., Liu, X.-Y., Huo, F.-Q., Li, H., Barry, D.M., Krieger, S., Kim, S., Jeffry, J., Liu, Z.-C., *et al.* (2014). Cross-inhibition of NMBR and GRPR signaling maintains normal histaminergic itch transmission. *The Journal of Neuroscience* *In press*.

Zhao, Z.Q., Huo, F.Q., Jeffry, J., Hampton, L., Demehri, S., Kim, S., Liu, X.Y., Barry, D.M., Wan, L., Liu, Z.C., *et al.* (2013). Chronic itch development in sensory neurons requires BRAF signaling pathways. *J Clin Invest* 123, 4769-4780.

Zhao, Z.Q., Scott, M., Chiechio, S., Wang, J.S., Renner, K.J., Gereau, R.W.t., Johnson, R.L., Deneris, E.S., and Chen, Z.F. (2006). Lmx1b is required for maintenance of central serotonergic neurons and mice lacking central serotonergic system exhibit normal locomotor activity. *J Neurosci* 26, 12781-12788.